St. Catherine University
SOPHIA

Antonian Scholars Honors Program

School of Humanities, Arts and Sciences

3-2014

Heart Failure and Design of Potentially Therapeutic Mutants Relieving SERCA Inhibition: Expression and Analysis of Phospholamban Mutants

Kristina R. Poss

Follow this and additional works at: https://sophia.stkate.edu/shas_honors

Part of the Organic Chemistry Commons

HEART FAILURE AND DESIGN OF POTENTIALLY THERAPEUTIC MUTANTS

RELIEVING SERCA INHIBITION: EXPRESSION AND ANALYSIS OF

PHOSPHOLAMBAN MUTANTS

By

Kristina R. Poss

A Senior Project in Partial Fulfillment of the Requirements of the Honors Program

ST. CATHERINE UNIVERSITY

March 13th, 2014

ACKWNOLEGEMENTS

I would like to acknowledge and thank those who helped to make this project possible:

Project Advisor:

      Dr. Kim Ha

Project Committee:

      Dr. Gina Mancini-Samuelson

      Dr. John Pellegrini

      Dr. James Wollack

University of Minnesota Genomics Center for DNA Sequencing

Dr. Gayle Gaskill, Antonian Scholars Honors Program

St. Catherine University Chemistry Department

TABLE OF CONTENTS

INTRODUCTION

Heart disease is the leading cause of death for both men and women in the U.S.[1] Yet, current treatment has varying degrees of success. In fact, ten percent of those with heart failure find no success with therapy or symptom management and are considered to have advanced heart failure.[2] Due to the prevalence and severity of heart disease, research to gain deeper understanding and promote opportunities for cardiovascular therapies are highly beneficial.

Improper calcium ion cycling is often the cause of heart failure.[3] The concentration of calcium ions impacts contraction and relaxation therefore investigating cardiac calcium cycling is valuable. A small protein in the sarcoplasmic reticulum (SR) membrane, phospholamban (PLN), impacts cardiac contractility as it plays a role in calcium ion cycling. Phospholamban is a known inhibitor of the sarco/endoplasmic reticulum Ca^{+2} ATPase pump (SERCA). Research seeks to more fully comprehend the composition, interactions, and physiological role of PLN; as well as design and investigate potentially therapeutic mutants of PLN. Mutants of PLN have been investigated as a target for gene therapy to prevent and treat heart failure. Ideal therapeutic mutants of PLN would modify PLN activity to in turn relieve some inhibition on SERCA. Given the current knowledge and revealing the significant physiological role of PLN, continued study of PLN is valuable as it will yield a greater understanding of cardiomyopathy, and holds cardiovascular therapeutic potential.

For this project I designed, cloned, expressed, and assessed rational mutants of phospholamban with the aim of therapeutic potential. The hope was to answer in part, or in full, several questions: 1) How might each of the rationally designed mutants affect the disorder and mobility of PLN? 2) Can the PLN mutants be effectively cloned, expressed, and purified? 3)

How do the PLN mutants interact with its main regulatory enzymes? 4) Do the PLN mutants meet the criteria for a PLN therapeutic mutant design?

Here, background related to PLN including structure, regulation by phosphorylation, and modulation of SERCA is detailed. Predictions and findings on properties and synthesis of rationally designed PLN mutants are also presented. Of the four mutants designed, the substitution of arginine with glutamic acid at position 14 (R14E), and glutamine substituted with glutamic acid at position 26 (Q26E) were able to be cloned, expressed, and purified. Findings suggest that R14E and Q26E are predicted to fit three out of the five criteria for PLN therapeutic mutant design as minimal change to secondary structure and increased disorder or mobility in domain 1a is predicted. Furthermore, this project highlights the usefulness of these bioinformatics databases to screen for potential mutants for study. Phospholamban is valuable to study and PLN mutants R14E and Q26E are promising for continued analysis to further answer the major questions. Continued study of these mutants could offer insight into the interaction between SERCA and PLN, and to potential treatments for heart failure.

BACKGROUND

Heart Disease and Treatment

There were over one million hospitalizations for congestive heart failure (CHF) in 2010 alone, and it is estimated that 5.8 million people in the United States have CHF.[4] Heart failure is characterized by an insufficient amount of blood pumped by the heart for the needs of the body. The heart compensates for failure in several ways: such as enlarging by stretching or increasing muscle mass, and pumping faster. These compensations lead to many of the common symptoms of heart failure, including shortness of breath, fluid build-up, and increased heart rate.[2]

One of the most common types of CHF is idiopathic dilated cardiomyopathy, which affects 40 out of 100,000 in the population.[3] Idiopathic dilated cardiomyopathy can be caused by a specific PLN mutation where arginine at position nine is substituted with cysteine. The disease is characterized by left ventricular dilation and systolic dysfunction. The left ventricle pumps oxygen rich blood from the atrium to the rest of the body. When the left ventricle is enlarged, less blood is able to be pumped, resulting in less volume of oxygenated blood to the rest of the body. [2] Systolic dysfunction results in an inability of the ventricles to contract normally, thus less volume of blood enters circulation. A decrease in the volume of oxygenated blood to the rest of the body can be damaging as it is inadequate for the needs of other organs and biological processes.

Current prevention and treatment of heart failure as outlined by the American Heart Associate include lifestyle changes, medications, and surgery.[2] Depending on the severity of heart failure and the damage, these treatments have varying success. Yet, ten percent of those with heart failure find no success with therapy or symptom management.

Due to the prevalence and severity of heart disease, research intended to gain deeper understanding and promote opportunities for cardiovascular therapeutic potential is highly beneficial. Gene therapy has been proposed as a promising method for the treatment of heart failure as it has the potential to affect biological processes impacting heart failure.[5] Gene therapy is the use of genes, delivered via a carrier called a vector, to treat or prevent disease.[6] The vector containing the therapeutic gene can be delivered intravenously, or directly into tissue. Gene therapy either introduces a new gene, or replaces a mutated one with a healthy gene, to produce a functional protein as a means to treat or prevent disease.

Calcium Ion Cycling and SERCA

Often, calcium ion handling in heart muscle cells is a cause of heart failure; therefore, calcium ion handling is a worthwhile gene therapy target to investigate.[3] Calcium ion cycling is crucial to cardiac muscle function as it signals muscle contraction and relaxation. A defect in cycling affects the rate and strength of contraction and relaxation. The sarcoplasmic reticulum (SR) is a membranous network of tubes surrounding each myofibril, and it stores intracellular calcium ions. Calcium ion pumps are located on the SR membrane, allowing for the release and re-uptake of calcium ions by the SR. This calcium ion cycling is closely regulated as calcium concentration in the cytoplasm of a muscle cell signals either muscle contraction or relaxation.[7]

The presence of calcium activates contractile proteins, and when the concentration of calcium ions in the cytoplasm is high, the calcium ions bind to troponin C of the troponin protein complex.[8] When a large amount of calcium, around 1 μM, is present in the cytosol, calcium can bind to troponin causing the removal of the tropomyosin blockade, exposing the binding sites for the myosin heads on the actin filaments.[9,10] Upon the binding of calcium ions, troponin shifts its position, therefore moving the attached protein tropomyosin, which is coiled around the protein actin. Before the shift, tropomyosin blocks the myosin binding sites on actin. After the shift, which was due to the binding of the calcium ion, the myosin binding site on actin is available (Figure 1). The myosin head is then able to bind to the newly exposed sites on actin. Muscle contraction occurs as the energy molecule adenosine triphosphate (ATP) forms a bond with myosin, causing myosin to release from actin. Then, as ATP is hydrolyzed to adenosine diphosphate (ADP) and phosphate, the energy produced bends the myosin protein head back, to loosely bind to the next site on actin. As the inorganic phosphate is released, the myosin head pushes on actin, providing a power-stroke, and then releases ADP. The cycle can then begin again, and continue, with the binding of another ATP molecule. However, as the cytosolic

concentration of calcium decreases to around 100nM calcium ions are removed from troponin. This allows tropomyosin to bind and cover the myosin binding sites on the actin filaments—and relaxation occurs.
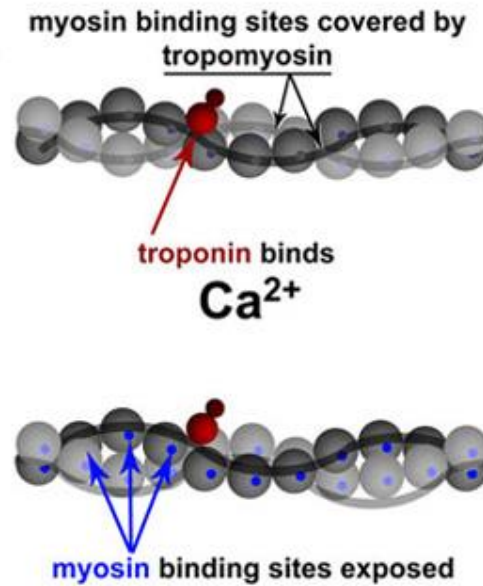

Figure 1: Binding of calcium ion to troponin.[11] As calcium ions bind, the myosin binding sites previously covered by tropomyosin are exposed allowing for contraction.

Relaxation occurs by the re-uptake of the calcium ions into the SR by the SERCA pump, also referred to as the calcium pump.[12] In Figure 2, SERCA is shown in the SR membrane associated with PLN. SERCA pumps two calcium ions from the cytosol into the SR by ATP hydrolysis, altering the concentration of calcium in the cytosol, and thus affecting the strength and rate of contraction and relaxation.[13] In fact, 75% of the calcium ions are removed from the cytosol by SERCA, and 25% are removed by the sodium/calcium exchanger.[14] The inability to remove cytosolic calcium ions, such as by one of these pumps in the cell membrane, decreases the amount of calcium ions loaded into the SR, resulting in impaired systolic function in

subsequent contractions.[5] The SR is the main source of calcium ions for cardiac myocytes.

Often, a defect in calcium ion cycling is related to an inadequate calcium ion store in the SR.[15]

With a smaller store of calcium ions to be released for the next contraction, cardiac contractility,

or the strength of the contraction, is reduced. Reduced cardiac contractility characterizes heart

failure and as a result, leads to irregular or insufficient contraction of the cardiac muscle.

Therefore, the activity of SERCA is important to normal cardiac contractility. In fact, studies

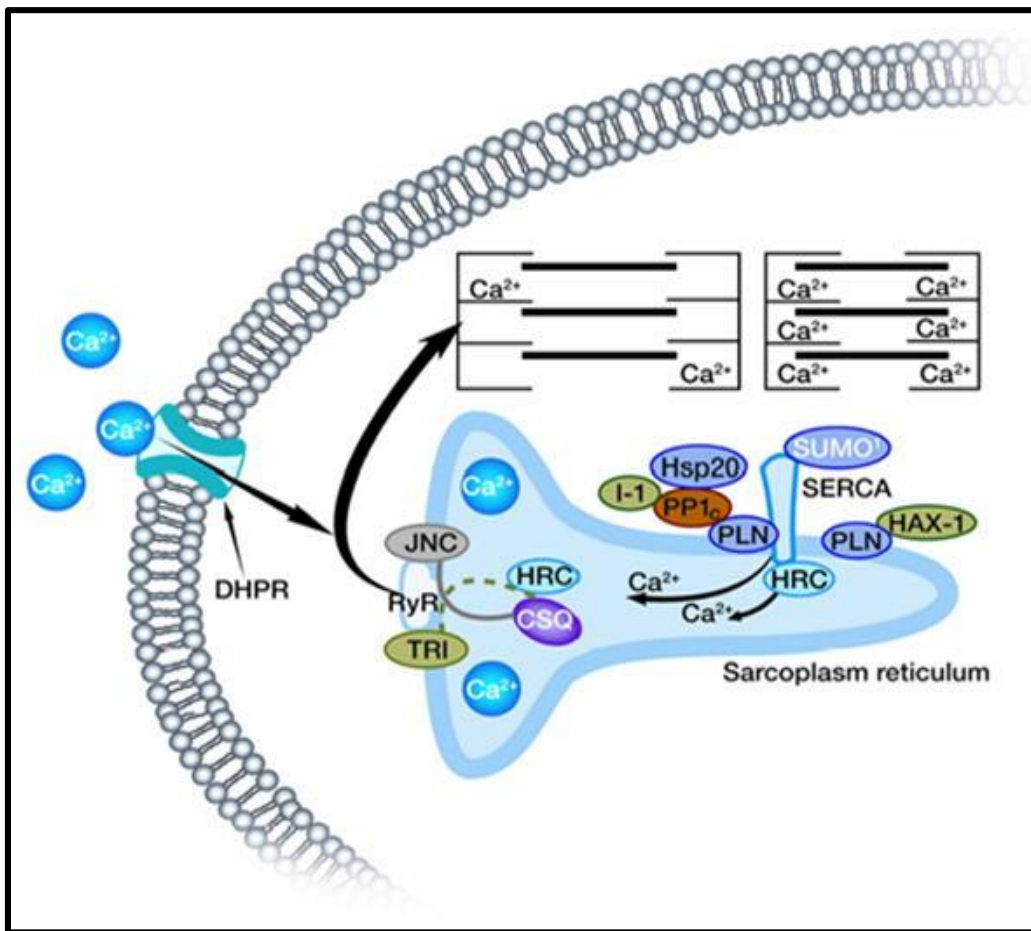have found that in human heart failure the average activity of SERCA is reduced.[12]

Figure 2: Calcium cycling.[16] Calcium is released by RyR and binds to troponin on the myofibril

allowing for contraction. Calcium is re-uptaken into the SR by SERCA as regulated by PLN,

allowing for relaxation.

Phospholamban, a Regulator of SERCA

Since the activity of SERCA is crucial to cardiac contractility, factors that influence the activity of SERCA are important to consider. One of the main regulators of SERCA is a small protein contained in the SR membrane, phospholamban (PLN) (Figure 3). Phospholamban allosterically regulates SERCA, meaning PLN interacts with SERCA at a site other than the enzyme active site.[13] Through interaction with PLN the structure of SERCA is altered and this change impacts the affinity of SERCA for calcium ions. In turn, the activity of the pump and subsequent contraction and relaxation is affected. The change in structure and interactions translates to a change in function. The structure-function relationship is key to biological systems for several reasons, one being that it allows for regulation.
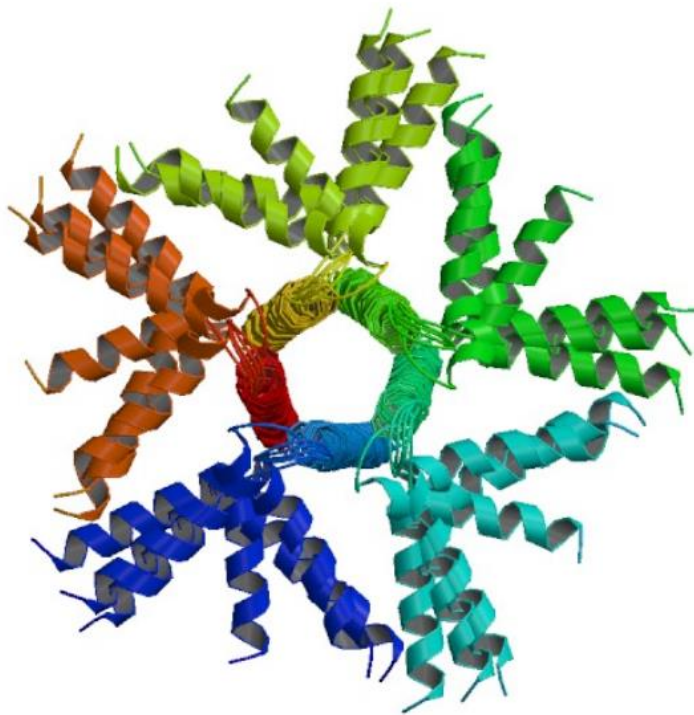

Figure 3: Phospholamban ribbon image.[17] The pentamer of five α-helices is shown in ribbon form with each α-helix identified by a different color.

The change in interaction between PLN and SERCA is based on the phosphorylation state of PLN: whether PLN is phosphorylated or dephosphorylated. Proteins have a hierarchical structure that can be altered when a protein is modified, and this change in structure affects the function. Phospholamban is regulated by modification with a phosphate group (PO_4^{-3}). The enzyme protein kinase A (PKA) phosphorylates, meaning it adds a phosphate group. When a phosphate group is added it affects the structure of the protein due to changes in interactions, charge and/or spatial arrangement. Specifically, when PLN is phosphorylated the change in structure relieves inhibition on SERCA, allowing for more calcium ions to be pumped into the SR. Therefore, cardiac contractility is increased because the removal of the calcium ions from the cytosol into the SR increases the available calcium ion store for the next cardiac cycle.

When the phosphate group is removed by the enzyme protein-phosphotase-1 (PP1), the structure of PLN changes. Dephosphorylated PLN inhibits the activity of SERCA, decreasing the number of calcium ions pumped into the SR, resulting in a decrease in the strength of subsequent contractions because of the decreased availability of calcium ions.[18] Phospholamban interacts and allosterically regulates SERCA by impacting the affinity of SERCA for calcium ions, and as a result, affecting cardiac contractility.

Studies support the link between PLN inhibition of SERCA and heart failure. In human heart failure it has been found that SERCA levels are typically low, resulting in a high ratio of PLN to SERCA.[19] The higher the ratio, the greater the inhibition on SERCA, causing lower calcium affinity. Less calcium affinity results in less calcium reuptake into the SR; so less calcium is available for the next contraction. Additionally, researchers have found significantly decreased amounts of phosphorylated PLN in patients with heart failure. [19] Consequently,

higher amounts of dephosphorylated PLN are present, inhibiting SERCA. Clearly, PLN is related to heart failure by its modulation of SERCA activity.

With a link to heart failure, PLN has and continues to be studied to learn more about the interaction with SERCA in hopes to identify potential therapeutic options. The structure of proteins can be manipulated to observe the functional impact of the change and to offer further insight into the nature of the interaction or function. One way the structure can be altered is by changing a specific amino acid using site-directed mutagenesis. The resulting DNA is a mutant, and the resulting protein is different. Studies altering the primary structure of a protein, the amino acid sequence, of PLN and observing the physiological impact have been performed. The findings support the impact of PLN on cardiac contractility. In fact, studies of super-inhibitory mutants of PLN in mouse models suggest that PLN impairs cardiac function.[12] Furthermore, mice deficient in PLN were studied and showed increased contraction and relaxation function, as well as an increase in the affinity of SERCA for calcium ions.[20] PLN is clearly linked to cardiac contractility and heart failure.

Several PLN mutants are notable for having an impact on cardiac contractility. For instance, Iwanaga et al. have executed studies on a PLN mutant where serine at position 16 has been substituted with glutamic acid (S16E), which mimics the phosphorylated state and therefore does not inhibit SERCA.[5] It is thought that in the S16E PLN mutant, part of the cytoplasmic domain unfolds to a similar degree that PLN unfolds when phosphorylated, therefore relieving inhibition on SERCA.[21] Also, this mutant likely competes with wild-type PLN for interaction with SERCA. Use of S16E PLN in rat models showed improved left ventricular function in rats with myocardial infarction.[5] Competition and assay data utilizing cardiac cells support these findings showing that PLN mutant S16E can compete with wild-type PLN. Therefore, S16E

PLN has an ability to interact with SERCA, and alter its activity.[21] Furthermore, S16E PLN administered in gene therapy has shown to reverse heart failure in sheep.[22] In fact, adeno-associated-virus-mediated gene therapy to overexpress SERCA or inhibit PLN continue to be investigated in in-vivo and clinical trials in humans.[9] These results suggest that the success found in the animal models to prevent heart failure and heart failure progression could be effective to prevent or treat heart failure in humans via gene therapy.

A second noteworthy PLN mutant is a human genetic mutation where arginine at position nine is replaced by cysteine (R9C) and is known to cause heart failure. It is thought that this mutant has an inability to be phosphorylated at serine 16, therefore SERCA inhibition cannot be relieved, likely contributing to a decrease in contractility and therefore heart failure progression.[5] These research findings on PLN mutants, among others, demonstrate the ability to affect the function of SERCA through the dynamics of PLN.[13]

Assessing the outcome of altering the primary structure of the protein offers insight as to which amino acids are important to the function and interactions of the protein. Therefore, rationally designed PLN mutants are useful to investigate for potential therapeutic use. Since phosphorylated PLN relieves inhibition on SERCA allowing improved cardiac contractility, mutants are often designed to mimic the phosphorylated state, which is characterized by possession of increased structural dynamics.

Structure and Properties of Phospholamban

Phospholamban is a relatively small protein: around 6 kDa and composed of fifty-two amino acids in its monomeric form.[7] The structure of PLN is shown in Figure 4 and the sequence of amino acids for wild-type phospholamban is shown in Figure 5. It is a transmembrane protein of the SR, meaning it is bound in the SR membrane, of cardiac and

smooth muscle. The SR is one of two membranes surrounding each myofibril and is involved in

muscle contraction and relaxation as it serves as a calcium ion store.[23] Proteins, calcium pumps,
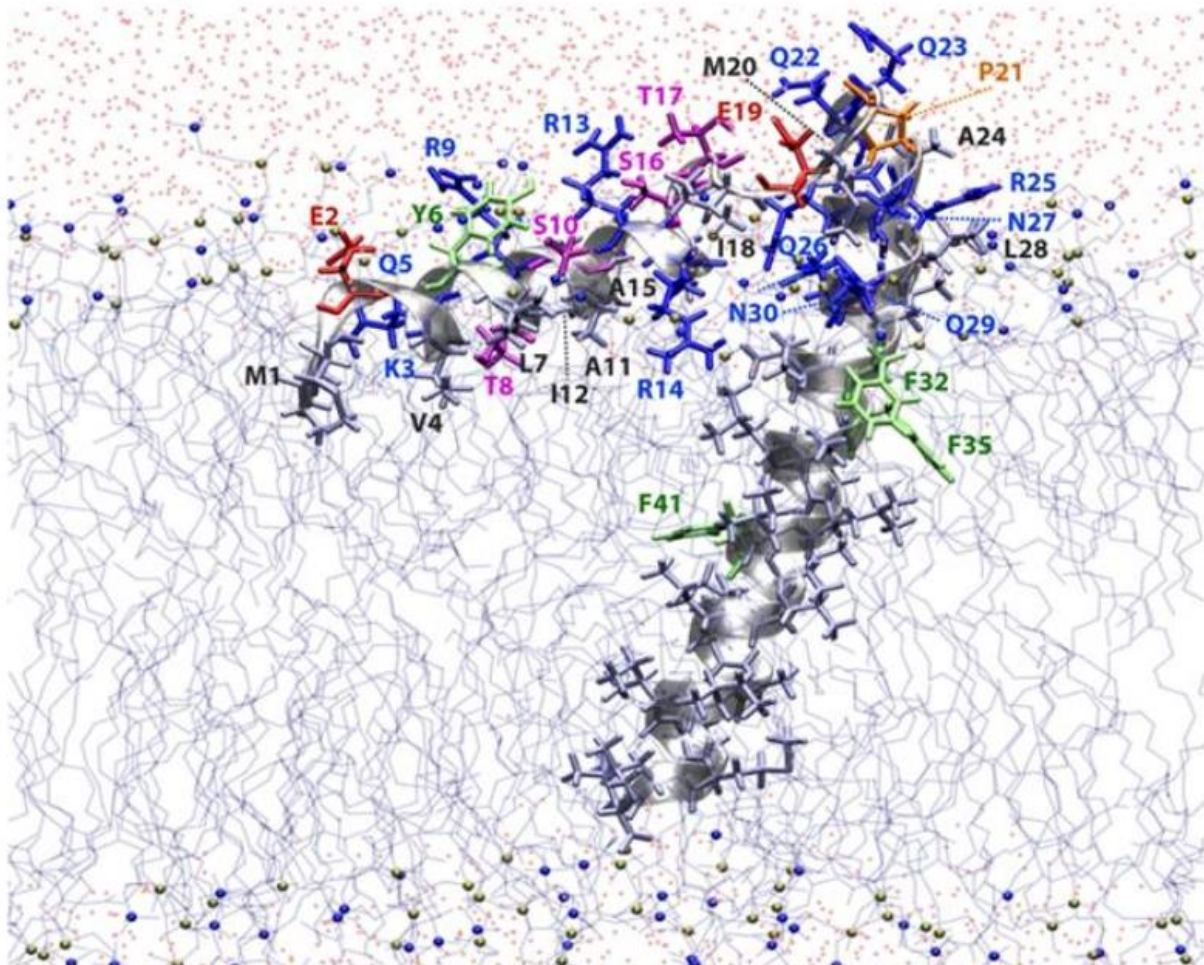
and calcium channels compose the SR.[24]

Figure 4: Structure of PLN illustrating spatial arrangement of amino acids.[31]

WT PLN: MEKVQYLTRSAIRRASTIEMPQQARQNLQNLFINFCLILICLLLICIIVMLL

Figure 5: Amino acid sequence of wild-type phospholamban (WT PLN).

Phospholamban is classified as a type II membrane protein as it is anchored to the SR

membrane via its C-terminus.[25] This largely hydrophobic protein has a secondary structure

consisting of a left-handed coiled-coil. Phospholamban is a monomer when dephosphorylated

yet, when phosphorylated five monomers aggregate to form a 30 kDa pentamer (Figure 3). It

possesses a high level of symmetry and is composed of five trans-membrane α-helices connected
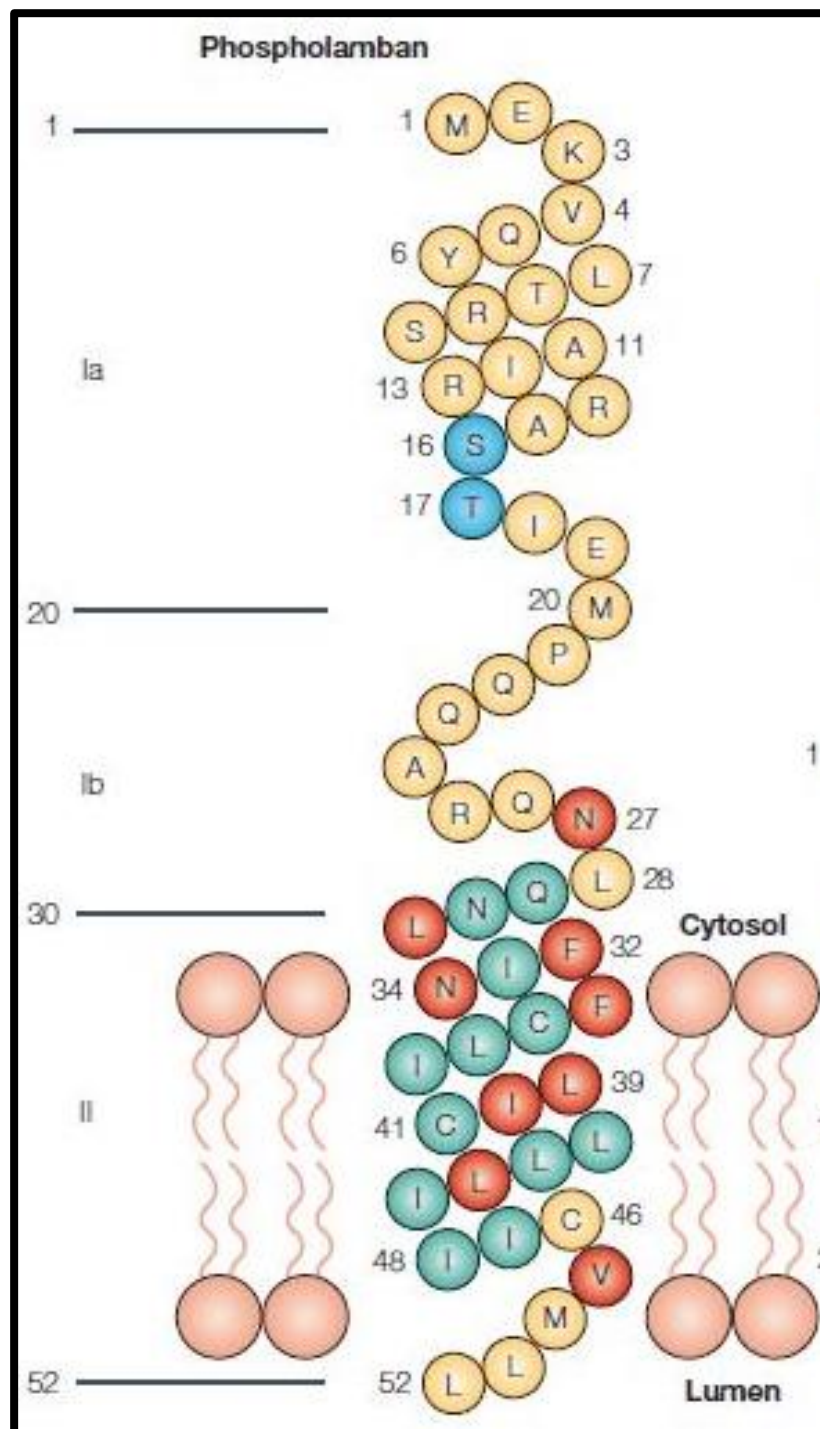
to one cytoplasmic α-helix via β-sheets.

Figure 6: Phospholamban amino acid diagram.[19] Each amino acid residue in the primary sequence of PLN is depicted. The amino acid number and the three domains are indicated on the left-hand side. The two blue residues indicate phosphorylation sites (S16 and T17).

Three distinct domains comprise a phospholamban monomer; each with unique properties contributing to the function of the protein. Figure 6 provides a schematic of these domains—Ia, Ib, and II. The first domain is a hydrophilic region at the amino terminal, labeled "Ia" in Figure 6, and is known as the cytoplasmic domain.[24] This area, consisting of 22 amino acids is highly charged as it is composed of mostly basic residues. The cytoplasmic domain contains the two phosphorylation sites, serine at position 16 and threonine at 17. Phosphorylation and dephosphorylation of these residues allows for the regulation of PLN activity. Both serine 16 and threonine 17 are oriented outward in 3-dimensional space, facilitating phosphorylation. The secondary structure of the cytoplasmic domain is an amphipathic helix, with the hydrophilic residues on one face, and the hydrophobic residues on the other face—this arrangement is known to be important for interactions and order. [26]

The next domain is the juxtamembrane region, labeled "Ib" in Figure 6. The juxtamembrane region includes the amino acids between proline 21 and lysine 27. One notable aspect is the presence of three glutamine residues, with the polar hydrophilic R groups oriented inside the helix.[24] Another significant feature of the juxta-membrane region is proline at location 21, as this outward facing residue acts as a hinge and allows a shape change when PLN is phosphorylated at serine 16 and threonine 17.

The last domain is the oligomer at the carboxylic acid terminal, labeled "II" in Figure 6. This region is largely hydrophobic as the twenty-five amino acids are integrated into the SR membrane. [7] The overall hydrophobicity allows for this part of the protein to span the

hydrophobic membrane. This region contains three cysteine residues. Cysteine possesses a unique ability to form a disulfide bond via the covalent linkage between its thiol group and the thiol group of another cysteine. Formation of disulfide bonds increase stability of the protein.

Another aspect of the structure of PLN to note is the amino acid at the C-terminus, leucine 52, is charged and actually extends into the inside of the SR.[24] In addition, the 3-dimensional structural model of PLN illustrates a pattern in the charge on the side of the alpha-helix of each monomer. The positively charged residues, including three arginine and a lysine, and the phosphorylation sites, serine and threonine, are mostly located on the same side of the α-helix.

Regulation of Phospholamban by Phosphorylation

The activity of PLN depends on its phosphorylation state. There are two important phosphorylation sites: one located at serine 16 and the other at threonine 17.[24] Both of these residues are located in the cytoplasmic domain and are facing outward on the α-helix for easy access for phosphorylation by globular kinases. When PLN is dephosphorylated it exists as a monomer and is associated with SERCA (Figure 7). Interaction between PLN and SERCA decreases SERCA's affinity for calcium ions, therefore inhibiting its function. [7] Therefore, when PLN is dephosphorylated, cardiac contractility decreases.

However, when PLN is phosphorylated, SERCA inhibition is relived. Five monomers of phosphorylated PLN may aggregate to form a pentamer upon phosphorylation (Figure 7).[16] However, there is debate on whether or not PLN completely dissociates from SERCA upon phosphorylation.[26] The result is an increased affinity of SERCA for calcium ions, therefore more calcium ions are pumped back into the SR. Consequently, more calcium ions are available

for the next contraction—allowing the increased cardiac contractility. Typically, about 50% of
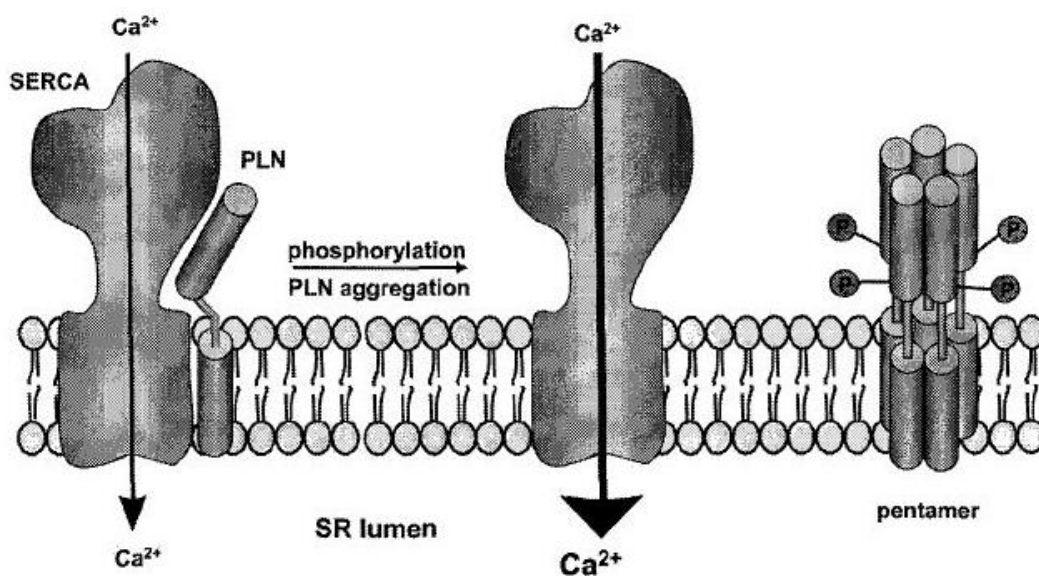
PLN is phosphorylated at any point in time.[12]

Figure 7: The structural effect of phosphorylation of phospholamban.[16] The left side of the graphic depicts dephosphorylated phospholamban, in its monomeric form, inhibiting SERCA. On the right side, phospholamban is phosphorylated, resulting in aggregation of five PLN monomers to form a pentamer, relieving inhibition of SERCA.

Phosphorylation site serine 16 is phosphorylated by cAMP-dependent protein kinase

(PKA) and threonine 17 is phosphorylated by Ca^{+2}-CAM –dependent kinase (CaMKII).[7]

Studies have demonstrated that serine 16 must be phosphorylated before threonine 17 can be

phosphorylated.[18] Conversely, phospholamban can be dephosphorylated at these sites by protein

phosphatase 1 (PP1) and small heat shock protein 20.[16]

One way phosphorylation is initiated is through a cascade of events beginning, with β-

adrenergic activation (Figure 8). Several signals ultimately lead to the phosphorylation of PLN

and the subsequent increase in active transport of calcium by SERCA. First, a β-agonist, such as

adrenaline is released in response to stress. [18] The β-adrenergic agonist activates β-adrenergic

receptors on the cell membrane of a muscle cell. The signal is transduced via G-proteins to stimulate the secondary messenger, adenylate cyclase, activity, producing cAMP. Presence of cAMP activates PKA and CaMKII, both enzymes that phosphorylate the proteins of the SR, and thus, PLN.[9,10] This results in an increase in cardiac output.
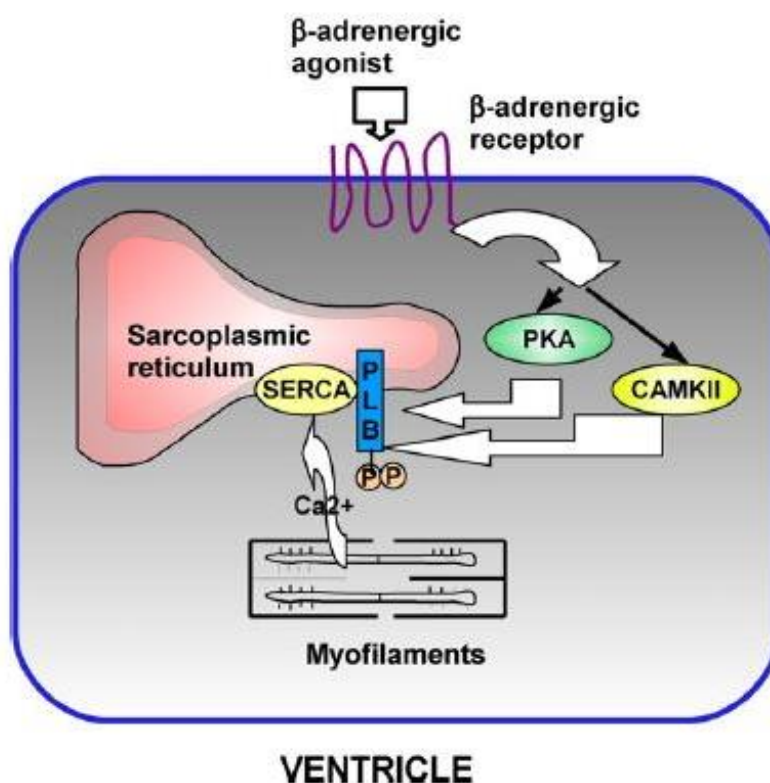

Figure 8: Mechanism of phosphorylation initiation by β-adrenergic agonist.[18] The release of a β-agonist begins a signal cascade resulting in the phosphorylation of PLN (labeled PLB in image) causing an increase in the rate of cell contraction and relaxation.

Phosphorylated and dephosphorylated PLN differ in structure in the degree of folding and unfolding.[26] When PLN is phosphorylated an order-disorder transition occurs.[13] Disorder is the lack of pattern or regularity in structure of the protein, such as the helix. Phosphorylation of PLN results in a negatively charged cytoplasmic domain, causing the helix to unwind. Specifically,

phosphorylation at serine 16 causes unfolding of the cytoplasmic region.[27] Regions of PLN that

fold and unfold are regions Ia, specifically amino acids 1-16, which is part of the cytoplasmic

domain, and Ib, amino acids 23-30, which is part of the trans-membrane domain. The

conformational changes disrupt the PLN-SERCA interaction, decreasing PLN activity and

relieving SERCA inhibition.[13]

If PLN is significantly or permanently dephosphorylated, or over expressed,

hypocontractility can result.[19] Hypophosphorylation of PLN has been linked to dilated

cardiomyopathy.[9] When PLN is dephosphorylated it inhibits SERCA activity, reducing calcium

ion affinity and thus decreasing the calcium ion reuptake into the SR. This results in less calcium

in the SR, impairing the next contraction and contributing to heart failure. Reduced contractility

decreases blood flow, which can be damaging to cells.

Several therapeutic approaches to heart failure by modifying PLN could be taken with an

overall goal to relieve SERCA inhibition and to increase cardiac contractility. These could

include decreasing PLN expression, increasing phosphorylated PLN, inhibiting PLN-SERCA

interaction, or designing a PLN mutant without function to compete with functional PLN.[13]

Decreasing PLN activity via inducing phosphorylation is currently being studied due to the

potential to treat heart failure.[19]

Criteria for Phospholamban Therapeutic Mutants

Tuning the structural dynamics of PLN has great therapeutic potential and criteria for

designing PLN mutants has been outlined.[28, 29] First, as discussed, increased structural dynamics

of PLN to mimic phosphorylated PLN is important. A mutant resembling phosphorylated PLN

has the potential to have the effect of phosphorylated PLN, alleviating SERCA inhibition.

Second, mutant PLN must be able to bind to SERCA in the same way as wild-type PLN. This is

important as the mutant PLN must be able to interact with SERCA to have potential to regulate

SERCA activity. Additionally, this will allow mutant PLN to compete with WT PLN. Another

aspect to consider when designing a therapeutic mutant of PLN is its ability to be

phosphorylated. By preserving the ability to be phosphorylated it could be useful to allow for

normal post-translational control. Additionally, the PLN mutant must result in a decreased

inhibition of SERCA. The aim of therapeutic PLN is to relieve, at least some, inhibition on

SERCA to allow more calcium ions to be pumped and stored to improve subsequent

contractility. Last, an inability to be dephosphorylated efficiently is an aspect to consider as

dephosphorylated PLN inhibits SERCA. Therefore, it would be beneficial to have more PLN

phosphorylated.

Project Overview

Using this information, four rationally designed PLN mutants were designed, and

predications about their impact on PLN were made. Then, bioinformatics databases were used to

predicted secondary structure, hydropathicity, and disorder. Next, polymerase chain reaction site-

directed mutagenesis was used to clone the mutants, and the sequence was confirmed with

Sanger DNA Sequencing. Then, BL21 E. coli cells were used to express the mutant proteins

which were purified by affinity chromatography.

RATIONALLY DESIGNED PHOSPHOLAMBAN MUTANTS AND HYPOTHESES

Glutamine at Position 5 Substituted with Arginine (Q5R)

Glutamine (Gln, Q)
MW: 128.14

Arginine (Arg, R)
MW: 156.19, pK$_a$ = 12.48
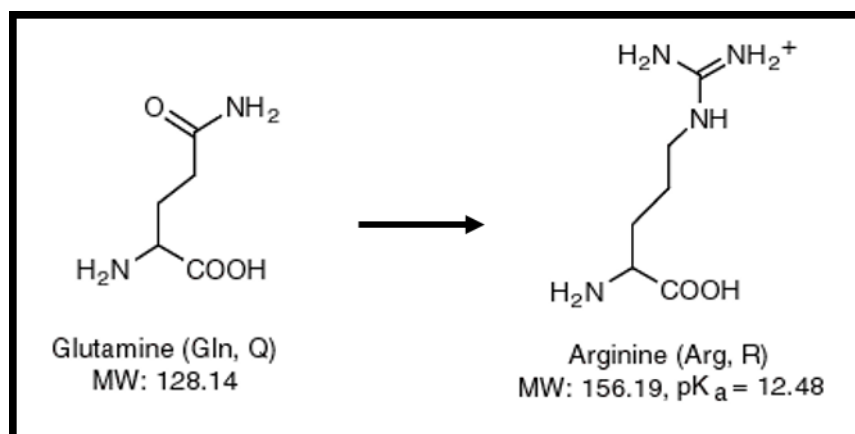
PLN mutant Q5R alters the charge in domain 1a. A change in charge in the cytoplasmic region is thought to disrupt PLN inhibitory function.[30] The change is from a polar, uncharged amino acid, to a positively charged amino acid. This could result in more interaction with the hydrophilic solution and less with the hydrophobic membrane—which could increase the flexibility of domain 1a. It is not likely mutant Q5R will affect V4 but it could hydrogen bond with Y6 or E2, and repel R9 (Figure 4). Additionally, this substitution results in a change in size as arginine is larger than glutamine, potentially causing further structural irregularity.

Glutamine at Position 5 Substituted with Isoleucine (Q5I)

Glutamine (Gln, Q)
MW: 128.14

Isoleucine (Ile, I)
MW: 113.16
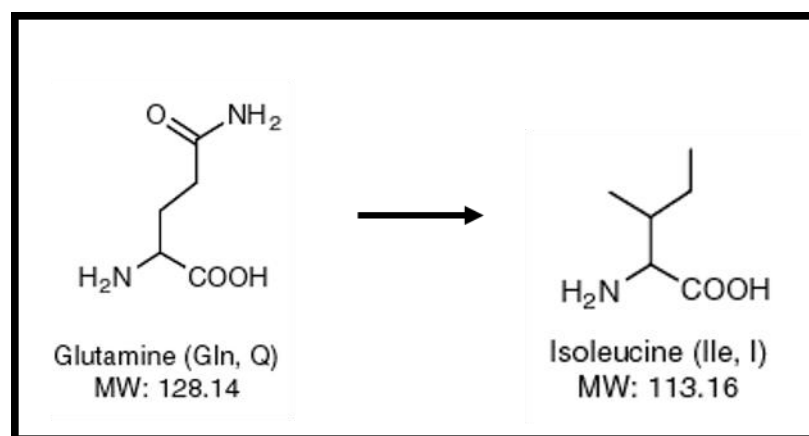
Mutant PLN Q5I was selected as the change from the polar to the hydrophobic residue will likely disrupt the domain 1a helix, and thus PLN inhibitory function. The interactions between residues will change as this mutation replaces a polar residue for a hydrophobic one.

This change likely will result in disruption of the amphipathic helix because of the change in hydropathicity. Therefore, this mutant may mimic the pseudo-phosphorylated state because research has demonstrated that the cytoplasmic helix of PLN is disrupted when PLN is phosphorylated.[32] Given the change to a hydrophobic residue at position 5, the mutant PLN may interact with the membrane more, increasing mobility and altering which face of the helix this residue is located. Also, this Q5I may interact or with V4, and repel E2, according to Figure 4. Additionally, Q5I would be interesting to compare and contrast with Q5R because the former is hydrophobic and the latter is hydrophilic.

Lysine at Position 3 Substituted with Glutamic Acid/Arginine at Position 14 Substituted with Glutamic Acid (K3E/R14E)
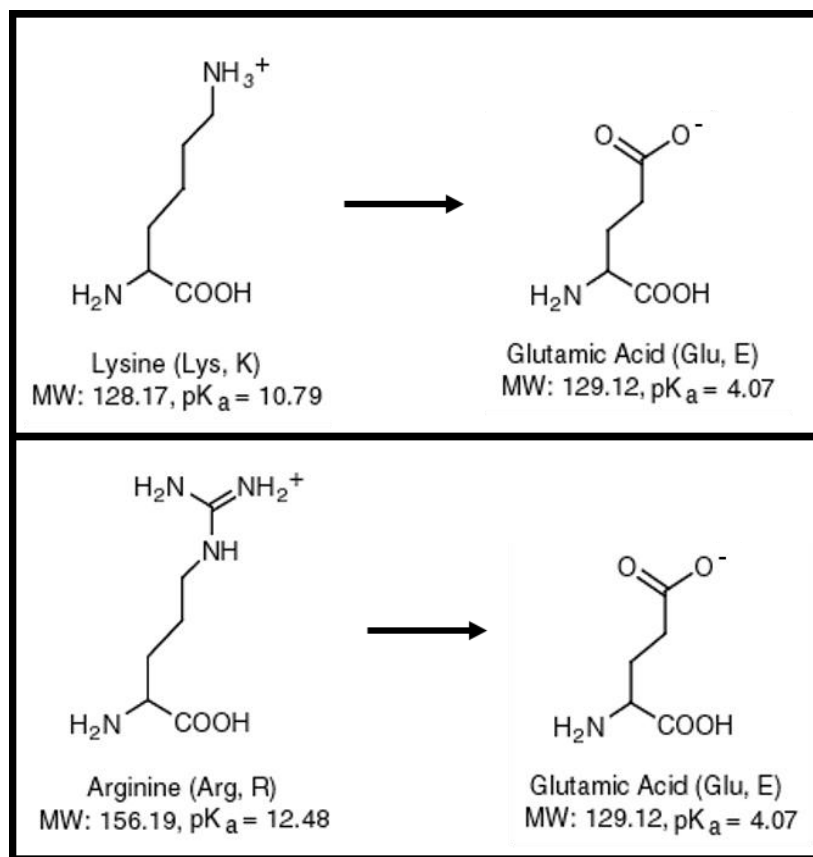
Studies measuring the affinity of SERCA for calcium ions have shown that charged and hydrophobic amino acids from glutamine at position two to isoleucine at position 18 are mutation sensitive in affecting the affinity of SERCA for calcium ions.[32] Furthermore, K3 and R14 have been identified as residues that not only interact with SERCA, but play a role in the inhibition of SERCA. Therefore, changing two charged residues likely will impact the affinity of SERCA for calcium ions. In fact, previous physiological studies of cardiac myocytes with K3E/R14E mutant showed a 45% increase in affinity of SERCA for calcium ions.[33] Furthermore, changing the charge will alter the electrostatic interactions and likely cause irregularity in the helix, which could mimic phosphorylation. Also, it is important to note that a mutation in this area likely has an impact on the ability of PLN to be phosphorylated by PKA because R14 is contained in the minimum recognition sequence for PKA. Therefore, it is important to learn more about this mutant. As the project progressed mutant R14E as a single mutant was focused on, which alone is a useful mutation and location for investigation. In fact, research has demonstrated that R14 deletion leads to dilated cardiomyopathy, providing support for the importance of this residue in SERCA regulation.[34]

Glutamine at Position 26 Substituted with Glutamic Acid (Q26E)

Glutamine (Gln, Q)
MW: 128.14

Glutamic Acid (Glu, E)
MW: 129.12, $pK_a = 4.07$
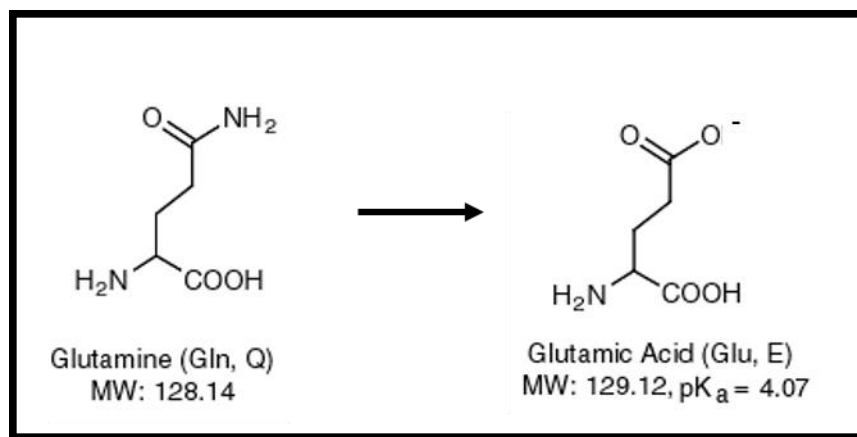
Residue 26 is a valuable place to investigate the effect of mutants as it swings away during phosphorylation.[35] Therefore, Q26 does not interact with SERCA when PLN is phosphorylated as the hydrogen bond between Arg324 of SERCA and Q26 of PLN is broken. This has been demonstrated as mutant Q26A results in the loss of PLN function, also suggesting the importance of the glutamine side chain for PLN inhibition.[30] Additionally, it is likely that residue 26 can impact the flexibility and mobility of PLN as it is near the P21 hinge. Therefore, changing from a polar to a charged amino acid likely will impact the mobility of PLN. The interaction with SERCA via hydrogen bonding may be altered due to this substitution, potentially relieving inhibition.

METHODS

Notes

Monomeric AFA PLN was utilized as the double stranded DNA in PCR vs. the pentameric WT PLN. The cysteines at locations 36, 41, and 46, are substituted with alanine, phenylalanine, and alanine respectively, in order to simplify the conditions and render PLN in its monomeric form for study (Figure 9). AFA PLN is suitable for this study as calcium ion activity assays demonstrate no significant difference in activity between WT PLN and AFA PLN.[36]

AFA PLN: MEKVQYLTRSAIRRASTIEMPQQARQNLQNLFINF**A**LILI**F**LLLI**A**IIVMLL

Figure 9: AFA PLN amino acid sequence.

Rationally Designing Therapeutic PLN Mutants

Due to the typical varying success in PCR, four mutants were designed—hoping at least one mutant would be successfully cloned. Four PLN mutants to further investigate for therapeutic consideration were carefully designed, and their potential impact on PLN was

hypothesized. While designing mutants, the five criteria for therapeutic mutant design were kept

in mind: increased structural dynamics to mimic phosphorylated PLN, an ability to bind to

SERCA the same as wild-type PLN, an ability to be phosphorylated, decreased inhibition of

SERCA, and an inability to be dephosphorylated efficiently. Since other successful mutants

mimic the phosphorylated state of PLN, the mutants rationally designed for this project also

focused on achieving a pseudo-phosphorylated state. Therefore, like the phosphorylated state, the

mutants were aimed at altering the structural dynamics—which can be done by altering the net

charge to disrupt the helix of domain 1a. Also, a change in the hinge region of the

juxtamembrane domain was considered in hopes to increase mobility. Additionally, it was hoped

to balance changing the disorder and mobility yet, a minimal change in secondary structure so

the mutants would still be able to interact with the main PLN regulatory enzymes.

Bioinformatics Analysis

Secondary structure, disorder, and hydropathicity were determined to be the three most

important properties to assess via bioinformatics databases. These three properties encompass the

key aspects of the criteria for a PLN therapeutic mutant design. Therefore, secondary structure,

hydropathicity, and disorder likely will offer insight into whether or not the mutant exhibits a

pseud-phosphorylated state. The amount of change in the secondary structure is helpful to predict

if there is a chance the mutant will be able to interact with the main regulatory enzymes. The

degree of disorder, or the regularity of the helix, will enable a reasonable prediction of whether

or not the mutant causes a disruption of the tertiary structure, and thus altering the dynamics.

Hydropathicity is important to assess as a change could cause more interaction with the solvent

or the membrane depending on the change—which would in turn impact the dynamics of PLN.

The bioinformatics tools were found and selected via searching and reviewing available databases. Secondary structure was analyzed by the Jpred3 database.[37] Hydropathcity was predicted using the peptide property calculator provided on the Innovagen website.[38] The disorder was predicted by DisEMBLE.[39] database. For each, the desired sequence of amino acids was entered and processed to obtain the predictions

Mutagenic Primer Design

Mutant DNA primers to be used in PCR site-directed mutagenesis were designed for each of the four rationally designed PLN mutants. Guidelines as outlined by the *QuikChange II Site-Directed Mutagenesis Kit* were followed. These guidelines included designing a primer between 25 and 45 bases in length, 10 to 15 bases on each side of the desired mutation, minimum guanine and cytosine base content of 40%, and a melting temperature of greater or equal to 78$^\text{o}$C. Melting temperature was estimated using

$$T_m = 81.5 + 0.41(\%GC) - \left(\frac{675}{N}\right) - \%mismatch$$

Where N is the total number of bases, and the %mismatch is the number of bases that changed, over the total number of bases. Different primers were measured against the criteria until the best fit was found for each mutant. The complementary base sequence was also determined, and both the forward and reverse sequences were ordered and obtained from Integrated DNA Technologies.

Cloning: Polymerase Chain Reaction Site-Directed Mutagenesis

Polymerase chain reaction (PCR) site-directed mutagenesis was used to attempt to clone the mutants. DNA mutant primers were obtained from Integrated DNA Technologies and each was diluted to 50μM with DI water. Then, a 1:5 dilution using 5μM of each solution was completed, resulting in a final concentration of 100ng/μL. Each reaction was prepared in a

separate micro-centrifuge tube, adding the reagents in the following order: deuterium-depleted water (40μL), reaction buffer (5μL), double stranded DNA (2μL, 100ng/μL), forward primer (1μL, 100ng/μL), reverse primer (1μL100ng/μL), dNTP (1μL). A corresponding control reaction for each mutation was prepared in a separate micro-centrifuge tube, adding reagents in the following order: deuterium-depleted water (42μL), reaction buffer (5μL), forward primer (1μL, 100ng/ μL), reverse primer (1μL100ng/ μL), dNTP (1μL). Next, the enzyme, Pfultra DNA polymerase was added (1μL, 2.5U/μL). The reactions were placed in the thermal cycler and cycled once at 95°C for 30s, and five times through the following cycle: 95°C for 30s, 55°C for 60 s, 68°C for 60s per kilo-base of plasmid. After the cycles were complete, of DpnI restriction enzyme (1μL,10U/μL) was added to each reaction and the reactions were incubated at 37°C for 60m. Next, gel electrophoresis in a 1% weight/volume agarose gel was ran for 60m at 100 volts to check the reaction. Samples ran were composed of the reaction (20μL) and ethidium bromide for stain (5μL). Once complete, the gel was imaged with UV light.

PCR Purification

The *GeneJET PCR Purification* kit and instructions were followed. A 1:1 volume of binding buffer (30μL) was added to the reaction (30μL) and mixed. The mixture was transferred to a purification column placed in a micro-centrifuge tube, centrifuged for 30-60s, and the flow-through was discarded. Wash buffer (700μL) was added and the reaction was again centrifuged for 30-60s, discarding the flow-through. The reaction was centrifuged for another 60s. Next, the purification column was transferred to a fresh 1.5mL micro-centrifuge tube and elution buffer (50μL) was added. The reaction was centrifuged for 60s and the flow-through was stored in a micro-centrifuge tube the refrigerator.

Transformation DH5-α E. coli with PCR Amplified DNA

DH5α E. *coli* (50μL) were thawed and aliquoted into micro-centrifuge tubes. Each

purified PCR reaction (10-15μL) was transferred into separate micro-centrifuge tube containing

the cells, using sterile technique. Sterile technique includes performing the transfer in proximity

of a lit Busen burner. The mixture was incubated on ice for 30m. Then, the reaction was heat

shocked in a water bath for 45s at 42°C to enable the DNA to be up-taken by the E. *coli* cells.

Using sterile technique, super optimal broth medium (500μL) was added to the reaction and the

reaction was incubated with shaking at 37°C for one hour. The reaction was centrifuged for 2m,

most of the supernatant was removed, and then the pellet was re-suspended. The mixture was

pipetted onto a sterile agar plate, under sterile conditions. The plate was incubated at 37°C

overnight and then observed for colony growth. Colonies that were present were inoculated by

growing the cells in a liquid broth media (LB) (5mL) overnight. Both a positive control with

pUC18, and a negative control, were made for a standard of comparison. The plasmids contained

a gene for ampicillin resistance and for maltose binding protein (MBP). (Heart Disease Fact

Sheet, 2013)

Plasmid Purification

The *GeneJET Plasmid Mini Prep Kit* instructions were followed to purify the expressed

plasmid. The solution containing LB and the colony grown overnight was transferred into an

eppendorf tube and centrifuged for 1m. This was repeated until all of the solution was

transferred. Then, the pellet was resuspended with resuspension solution (250μL), mixed well,

and vortexed. Next, lysis solution (250μL) was added and the tube was inverted 4-6 times to mix

thoroughly. Then, neutralization solution (350μL) was added and the tube was inverted 4-6 times

to mix. The solution was centrifuged for 5m, forming a white pellet. The supernatant was

transferred to the GeneJET spin column, centrifuged for 60s, and the flow through was

discarded. Next, wash solution (500μL) was added, the solution was centrifuged for 30-60s, and the flow through was discarded—this was repeated twice. To remove all excess wash buffer the solution was centrifuged for another 60s. The column was transferred to a clean 1.5mL micro-centrifuge tube. Then elution buffer (50μL) was carefully added and the solution was incubated for 2m at room temperature, then centrifuged for 2m. The plasmid DNA was stored in the micro-centrifuge tube at -20°C.

Quantification of Plasmid

UV-vis spectroscopy was used to measure the absorbance of the 1:11 diluted sample at 260nm. Using Beer's law $A = \varepsilon c l$—where A is the absorbance, ε is the molar absorptivity constant, l is the path length, and c is the concentration—the concentration of the sample can be calculated. The extinction coefficient for double stranded DNA is $0.02 \text{ M}^{-1} \text{ cm}^{-1}$. The samples with the known concentration were sent for Sanger DNA sequencing at the University of Minnesota. The sample included plasmid (5μL), primer (4μL), and water (3μL).

Transformation of BL21 E. coli **with Plasmid**

BL21 E. *coli* cells (50μL) were thawed and aliquot into micro-centrifuge tubes. The purified plasmid (100ng) was transferred into the micro-centrifuge tube containing the cells, using sterile technique. The mixture was incubated on ice for 30m. Then, the reaction was heat shocked in the water bath for 45s at 42°C to enable the plasmid to be up-taken by the E. *coli* cells. Using sterile technique, super optimal broth medium (500μL) was added to the reaction. The reaction was incubated with shaking at 37°C for 1h. The micro-centrifuge tube was centrifuged for 2m, most of the supernatant was removed, and the pellet was re-suspended. The mixture was pipetted onto a sterile agar plate, using sterile technique. The plate was incubated at

37°C overnight and then observed for colony growth. Colonies that were present were inoculated by growing the cells in LB (5mL) overnight.

Protein Expression

The colony in LB media was mixed using sterile technique with autoclaved DI water (400mL), 5x LB (100mL), glucose (10mL), vitamin cocktail[40] (5mL), mineral cocktail[40] (2.5mL), and ampicillin (500µL). The vitamin cocktail[40] contains calcium pentothenate (1mg/L), biotin (1mg/L), folic acid (1mg/L), niacinamide (1mg/L), and pyridoxal phosphate (1mg/L). The mineral cocktail[40] is composed of 6 mg/L $CaCl_2$ (6 mg/L), $FeSO_4$ (6 mg/L), $MnCl_2$ (1 mg/L), $CoCl_2$ (0.8 mg/L), $ZnSO_4$ (0.7 mg/L), $CuCl_2$ (0.3mg/L), H_3BO_3 (0.02 mg/L), $(NH_4)_6MO_7O_{24}$ (0.25 mg/L), EDTA (5 mg/L). The solution was placed in the shaker and incubated at 37°C to grow the cells. The optical density at 600nm was checked using the Spectrophotometer to measure the progress of the reaction just under 2h and the reaction was allowed to proceed until an optical density of about one was reached, which was achieved at 3.5 hours. At this time, the cells were induced with isopropyl β-D-1-thiogalactopyranoside (IPTG) promoter (1 M) to induce transcription. The cells were incubated for 4.5 hours to allow for protein expression, then they were harvested by separation using centrifugation.

Protein Purification

PLB AFA-MBP lysis buffer was made containing phosphate buffered saline (PBS 500mL), lysozyme (20mg), 100% glycerol (2.5mL), triton-X (2.5mL), dithiothreitol (DTT 50µL, 1M), leupeptin (25µL, 10ng/mL in dd water), phenylmethylsulfonyl fluoride (PMSF, 2.5mL, 17.4mg/mL), and pepstantin A (250µL, 1mg/mL in ethanol). The lysis buffer was added to the cells, vortexed, and mixed well. The mixture was then blended for several minutes with a hand blender, and sonicated for 25m with an interval of 2s. Next, the solution was centrifuged at

12,000 RPM for 20m at 4⁰C. Meanwhile, an affinity column with amylose resin (25mL) and was

washed with 3x the volume of water (75mL), and 2 times the volume of PBS (50mL) to

equilibrate. Then, the solution was poured over the column. The column was washed with PBS,

and then eluted with maltose, PBS, and TEV protease to elute MBP-PLN from the column.

Samples of the supernatant, flow-through, wash, and elution were kept and run on an SDS PAGE

gel for 35m at 60 mA. The gel was placed in trichloroacetic acid for 10m when it was poured off.

The gel was stained with coomassie brilliant blue dye and rocked for 10m. Methanol and acetic

acid were used to de-stain the gel overnight.

Concentrating Protein Sample

The elution sample containing the protein was concentrated using a 10kDa filter in a

stirred ultrafiltration cell with nitrogen gas until the sample was concentrated to a total volume of

20mL. 5mL of the flow-through was kept as a blank, and the top of the column was stored frozen

at -20⁰C.

RESULTS

Bioinformatics Data

Secondary Structure: Jpred3.[37]

In comparison of the secondary structure as predicated by Jpred3, no significant changes

in the secondary structure or solvent accessibility are observed between each mutant and wild-

type PLN (Figure 10). The results show the secondary structure at each residue. In A) of figure

10, the two distinct helices connected by a random coil are observed in each sequence similar as

in wild-type PLN. Also, the prediction of burial with 25% solvent accessibility (Figure 10B) and

with 5% solvent accessibility (Figure 10C) are similar between each mutant and wild-type PLN.

These results illustrate predicted minimal, non-significant change in the secondary structure.
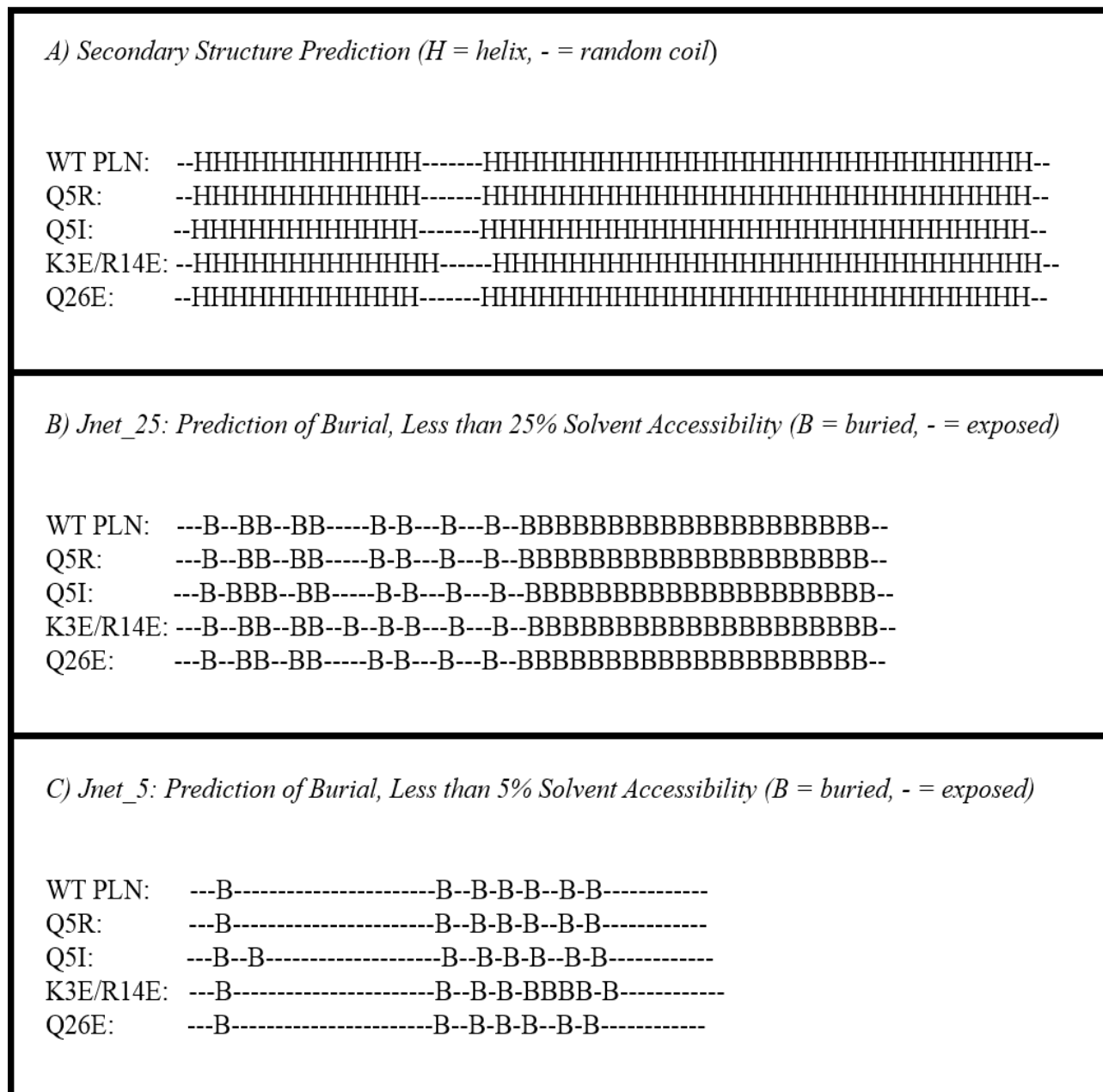
A) Secondary Structure Prediction (H = helix, - = random coil)


```
WT PLN:   --HHHHHHHHHHHH-------HHHHHHHHHHHHHHHHHHHHHHHHHHHHHH--
Q5R:       --HHHHHHHHHHH-------HHHHHHHHHHHHHHHHHHHHHHHHHHHHHHH--
Q5I:       --HHHHHHHHHHH-------HHHHHHHHHHHHHHHHHHHHHHHHHHHHHHH--
K3E/R14E: --HHHHHHHHHHHHH------HHHHHHHHHHHHHHHHHHHHHHHHHHHHHH--
Q26E:      --HHHHHHHHHHH-------HHHHHHHHHHHHHHHHHHHHHHHHHHHHHHH--
```

B) Jnet_25: Prediction of Burial, Less than 25% Solvent Accessibility (B = buried, - = exposed)


```
WT PLN:   ---B--BB--BB-----B-B---B---B--BBBBBBBBBBBBBBBBBBBB--
Q5R:       ---B--BB--BB-----B-B---B---B--BBBBBBBBBBBBBBBBBBBB--
Q5I:       ---B-BBB--BB-----B-B---B---B--BBBBBBBBBBBBBBBBBBBB--
K3E/R14E: ---B--BB--BB--B--B-B---B---B--BBBBBBBBBBBBBBBBBBBB--
Q26E:      ---B--BB--BB-----B-B---B---B--BBBBBBBBBBBBBBBBBBBB--
```

C) Jnet_5: Prediction of Burial, Less than 5% Solvent Accessibility (B = buried, - = exposed)


```
WT PLN:    ---B----------------------B--B-B-B--B-B------------
Q5R:        ---B----------------------B--B-B-B--B-B------------
Q5I:        ---B--B-------------------B--B-B-B--B-B------------
K3E/R14E:  ---B----------------------B--B-B-BBBB-B------------
Q26E:       ---B----------------------B--B-B-B--B-B------------
```

Figure 10: Secondary structure prediction and prediction of burial at each residue for WT PLN and each mutant by Jpred3 Database.[37]

Hydropathicity Analysis: Innovagen AB.[38]

Figure 11 shows the hydropathicity plot at each residue for wild-type PLN (A) and for each rationally designed PLN mutant (B-E). For mutant PLN Q5R (Figure 12B), both the wild-type and the mutant amino acid are hydrophilic, yet there is a change from a polar, slightly

hydrophilic glutamine, to a basic, charged, very hydrophilic arginine residue. Residue five for

mutant Q5I (C) changes from a polar, slightly hydrophilic glutamine to a aliphatic and

hydrophobic isoleucine—a more significant change. The double mutation K3E/R14E (D) shows

a change at both residue three and residue 14 from basic and hydrophilic, lysine and arginine, to

acidic and hydrophilic, glutamic acid. While these positions remained charged with the mutation,

the charge is positive in wild-type PLN, but negative in this mutant at locations three and 14.

Last, PLN mutant Q26E (E) is a mutation from a polar, slightly hydrophilic glutamine residue, to

a charged, acidic, more hydrophilic glutamic acid.
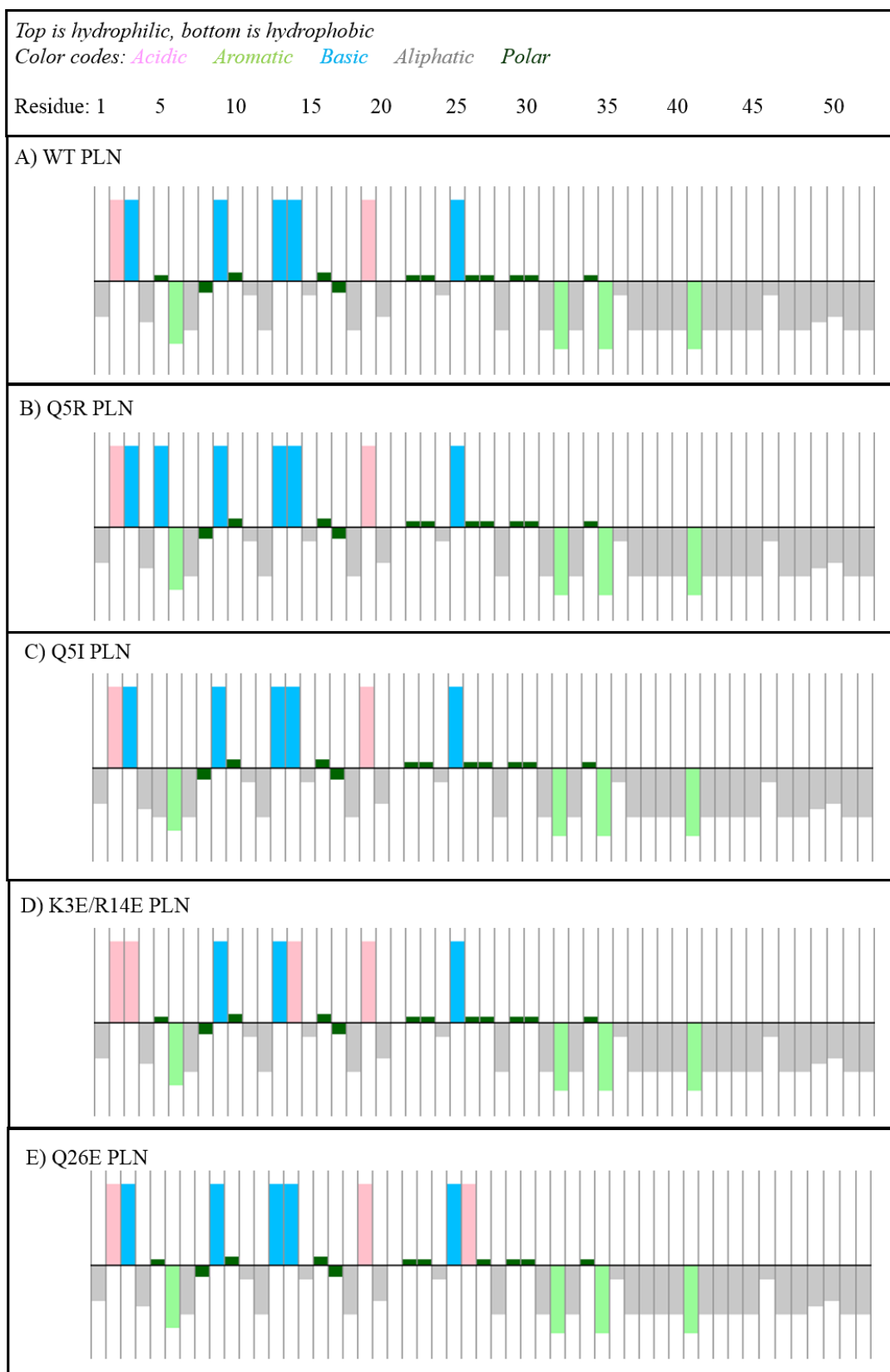
Figure 11: Comparison of Hydropathicity at Each Residue as Predicted by Innovagen AB. [38]

Further analysis of the hydropathicity of wild-type PLN and each PLN mutant is shown in figures 12 and 13. No significant difference was observed in the isoelectric point or net charge at pH 7 when comparing each Q5R PLN and Q5I PLN to wild-type PLN. The isoelectric point is just above 11, and the net charge at pH 7 is around three. Minimal predicted change in the isoelectric point and net charge at pH 7 was predicted between Q26E PLN and wild-type PLN. Mutant PLN Q26E is predicted to have a slightly lower isoelectric point, 10.38 vs. 11.22, and lower net charge at pH 7, two vs. three. PLN double mutant K3E/R14E demonstrated the greatest predicted change in isoelectric point and net charge at pH 7 compared to wild-type PLN. This mutant is predicted to have a significantly lower isoelectric point, 4.73 vs. 11.22, and lower net charge at pH 7, minus one vs. three.

Protein	Isoelectric Point	Net Charge at pH 7
WT PLN	11.22	3
Q5R PLN	11.83	4
Q5I PLN	11.22	3
K3E/R14E PLN	4.73	-1
Q26E PLN	10.38	2

Figure 12: Comparison of isoelectric point and net charge for WT PLN and PLN mutants as predicted by Innovagen AB.[38]

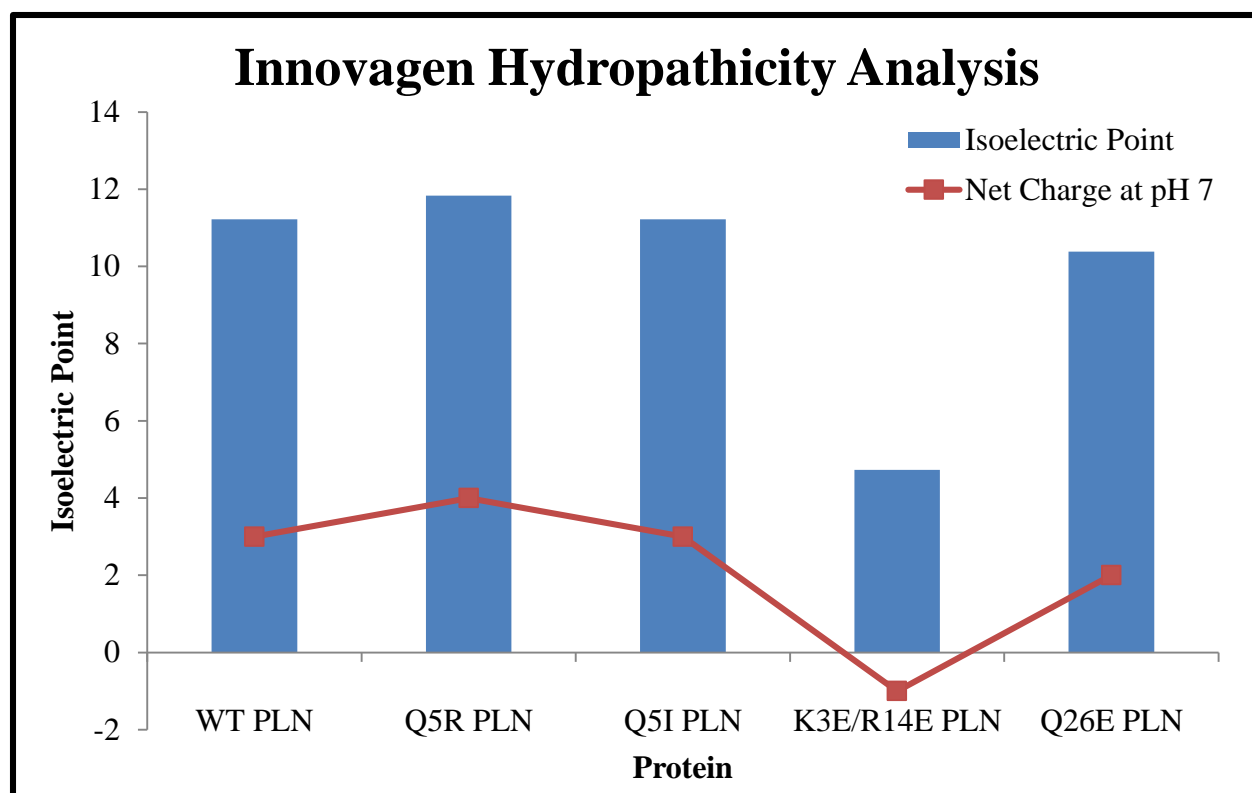## Innovagen Hydropathicity Analysis

Figure 13: Graphical comparison of isoelectric point and net charge for WT PLN and PLN mutants from Innovagen AB[38] data.

DisEMBLE.[39]

DisEMBLE is a database predicting the disorder of a protein based on an entered amino acid sequence. Two types of disorder are predicted: "loops", and "hot loops." Loops illustrates the predicted level of disorder based on where loops are present. This is significant because loops are the only areas where protein disorder exists, however, loops are not necessarily disordered. If loops are not disordered, they are ordered areas with either an alpha helix or beta-strand secondary structure. Hot Loops predicts loops with a high degree of mobility as loops that are highly dynamic exhibit disorder.

Disorder is exhibited in domain 1a, specifically between residues 15 and 22. Both phosphorylation sites, serine 16 and threonine 17, which exhibit disorder and increased mobility

upon phosphorylation, are in this range of predicted disorder (Figure 14 and 15). Furthermore, proline 21, which is believed to pivot like a hinge in wild-type phospholamban, and therefore is highly dynamic, is part of this high disorder range as predicted by DisEMBLE. This is also consistent with the secondary structure prediction by Jpred, which illustrates loops in this same region.

The Loops graph (Figure 14) shows that PLN mutant K3E/R14E is predicted to exhibit the greatest increase in disorder compared to wild-type PLN. PLN mutant Q26E is predicted to possess very similar disorder to that of wild-type PLN. Surprisingly, Loops has predicted that PLN mutant Q5I likely will have a decrease in disorder compared to wild-type PLN.

Hot loops prediction (Figure 15) illustrates a likely increase in structural dynamics for PLN mutants Q5R and Q26E. Double mutant K3E/R14E has been predicted by this method to have slightly less mobility compared to wild-type PLN. Additionally, wild-type PLN has a high probability of disorder from residues 10-20, while mutants Q5R, Q5I, and Q26E have this hot loops region expanded, beginning at residue one.

In both types of prediction, Loops and Hot Loops, the differences between wild-type PLN and a mutant are most apparent at the peak of disorder.
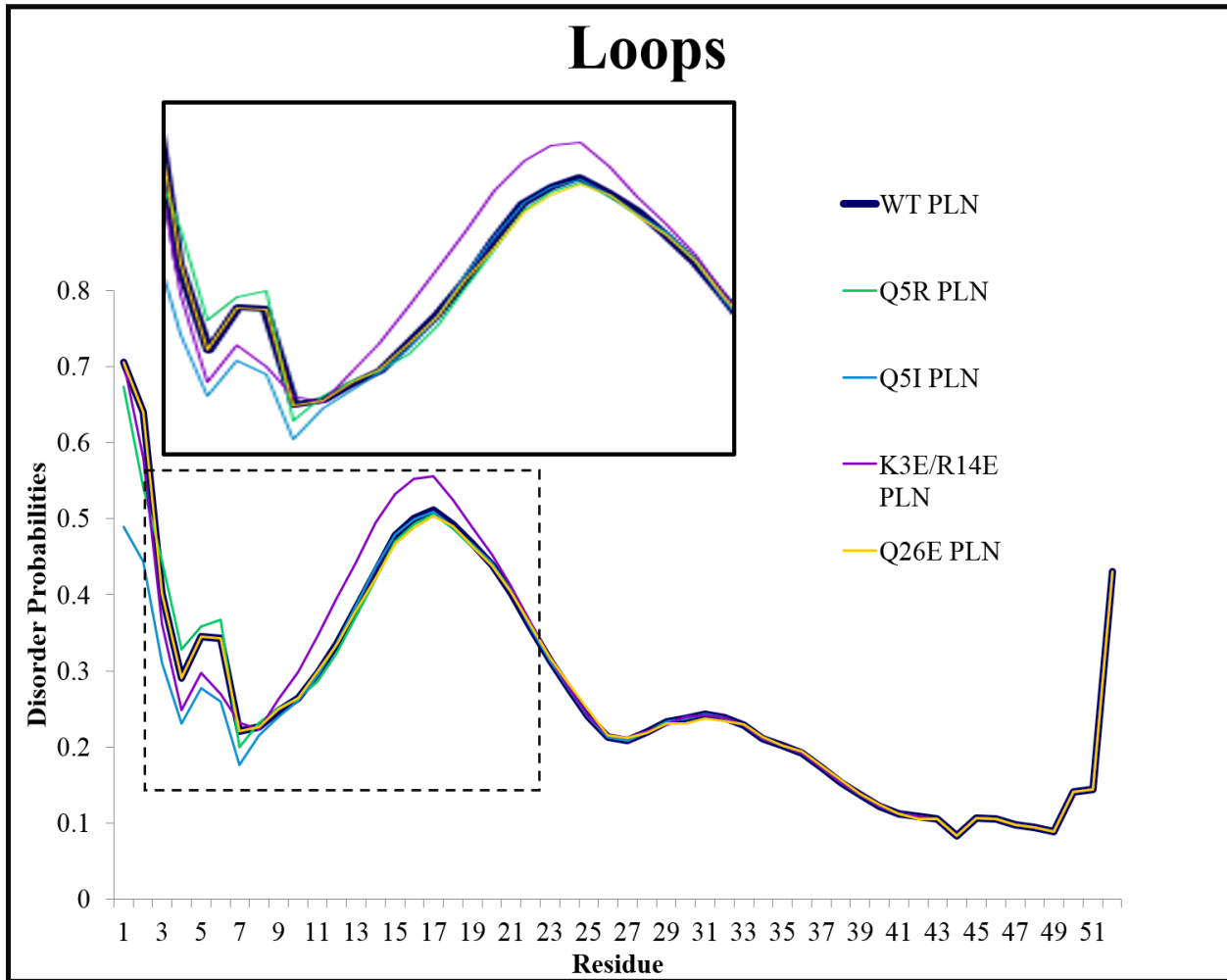
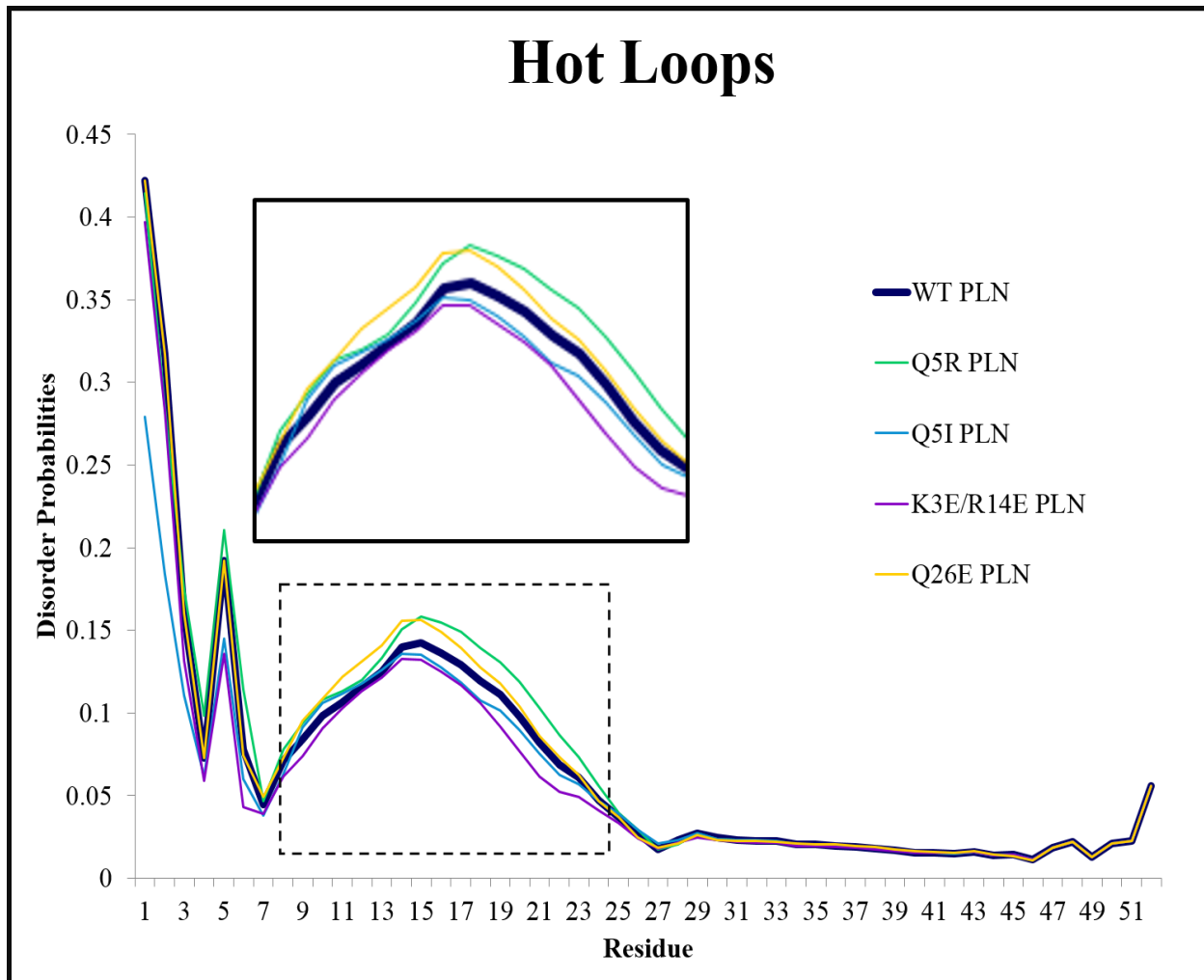*Figure 14: The Loops graph shows the probability of disorder as predicted by DisEMBLE.[39]*

Figure 15: The Hot Loops graph illustrates the probability of mobility as predicted by

DisEMBLE.[39]

Base Sequence of Designed Primers

Each letter represents a nucleic acid base: A-adenine, T-thiamine, C-cytosine, G-guanine.

*Bold is the mutation site in the sequence
*T_m is the calculated melting temperature (from method section "Mutagenic Primer Design")

Q5R PLN
1. 5' ATG GAA AAA GTG **CGC** TAT CTG ACC CGC AGC GCG 3'
2. 5' CGC GCT GCG GGT **CAG** ATA GCG CAC TTT TTC CAT 3'
$T_m = 78.6^oC$

Q5I PLN
1. 5' ATG GAA AAA GTG **ATT** TAT CTG ACC CGC AGC GCG ATT CGC CGC 3'
2. 5' GCG GCG AAT CGC **GCT** GCG GGT CAG ATA AAT CAC TTT TTC TAC 3'
$T_m = 79.7^oC$

K3E PLN
1. 5' ATG GAA **GAA** GTG CAG TAT CTG ACC CGC AGC GCG 3'
2. 5' CGC GCT **GCG** GGT CAG ATA CTG CAC TTC TTC CAT 3'
$T_m = 81.6^oC$

R14E PLN
1. 5' ACC CGC AGC GCG ATT CGC **GAA** GCG AGC ACC ATT 3'
2. 5' AAT GGT GCT CGC TTC GCG **AAT** CGC GCT GCG GGT 3'
$T_m = 79.3^oC$

Q26E PLN
1. 5' CAG CAG GCG CGC **GAA** AAC CTG CAG AAC CTG 3'
2. 5' CAG GTT CTG CAG **GTT** TTC GCG CGC CTG CTG 3'
$T_m = 78.3^oC$

Figure 16: PLN Mutant Designed Primer Base Sequences.

Gel Images after PCR

Figures 17 and 18 show an image of the gel ran after the completion of PCR for each designed PLN mutant, and a respective control. After PCR, the reaction was treated with the restriction enzyme Dpn-I. Dpn-I is a restriction enzyme that cleaves only methylated DNA, such as that produced by the E. coli. However, the recombinant DNA synthesized by PCR is not methylated, and therefore would not be cleaved. Therefore, the methylated DNA would be in fragments and travel farther on the gel than the uncut recombinant DNA. If any mutated DNA is present, a band that has travelled not as far as the digested product would be expected.

Samples showing two bands in the gel, which suggest a successful PCR, were purified to rid of remaining double stranded DNA. For the Q26E PLN reaction in figure 17 two bands are present, illustrating PCR product. The K3E PLN reaction also was potentially a successful PCR as there is a smeared band between the well and the digested product band. Some DNA remained in the well for both K3E and Q26E, which possibly could be product. Both were treated as successful PCR and the process was then continued with transformation.
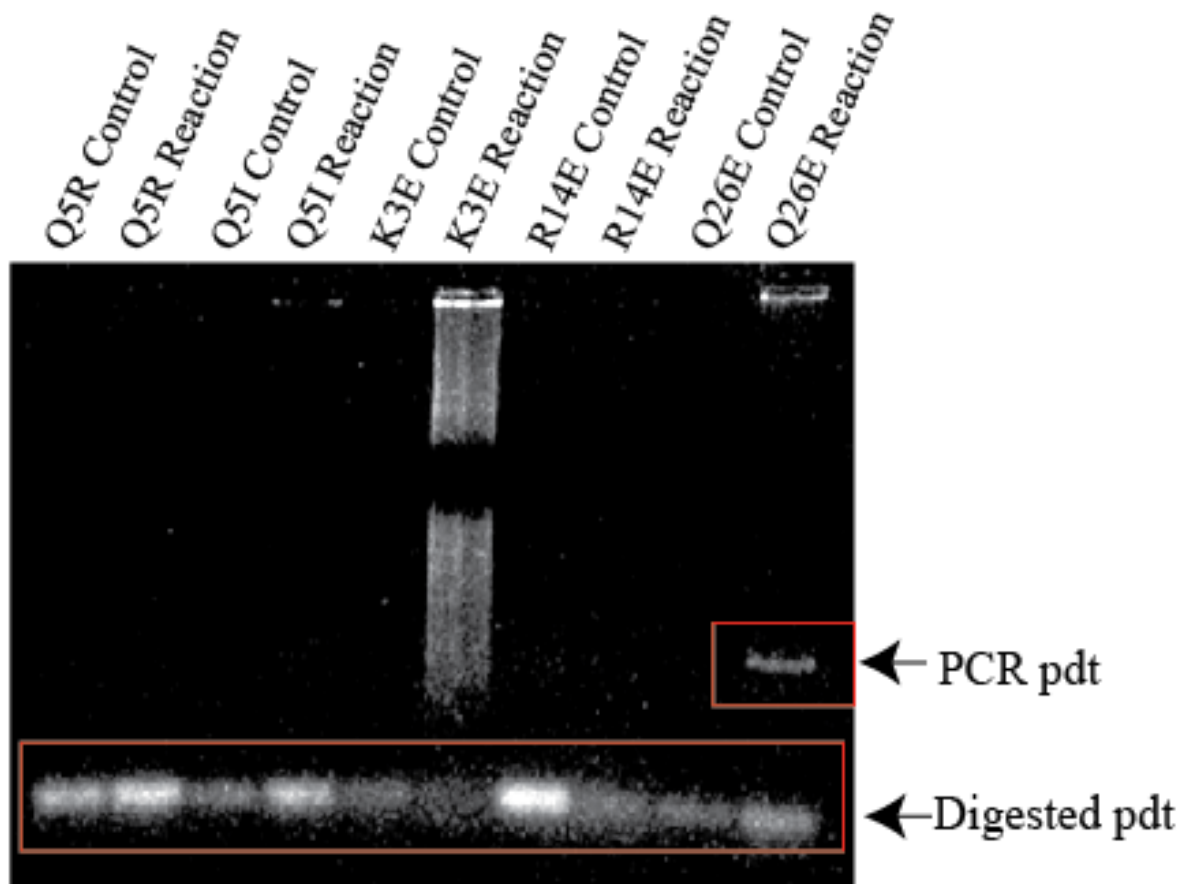

Figure 17: Gel image showing PCR product for Q26E and potentially for K3E.

Figure 18 is a gel image illustrating a successful PCR for Q26E PLN and R14E PLN, and a likely successful PC for K3E PLN. A second band is present for mutants Q26E PLN and R14E

PLN indicating digested DNA. The reaction lane for K3E PLN show a smeared band, suggesting the PCR might have worked.
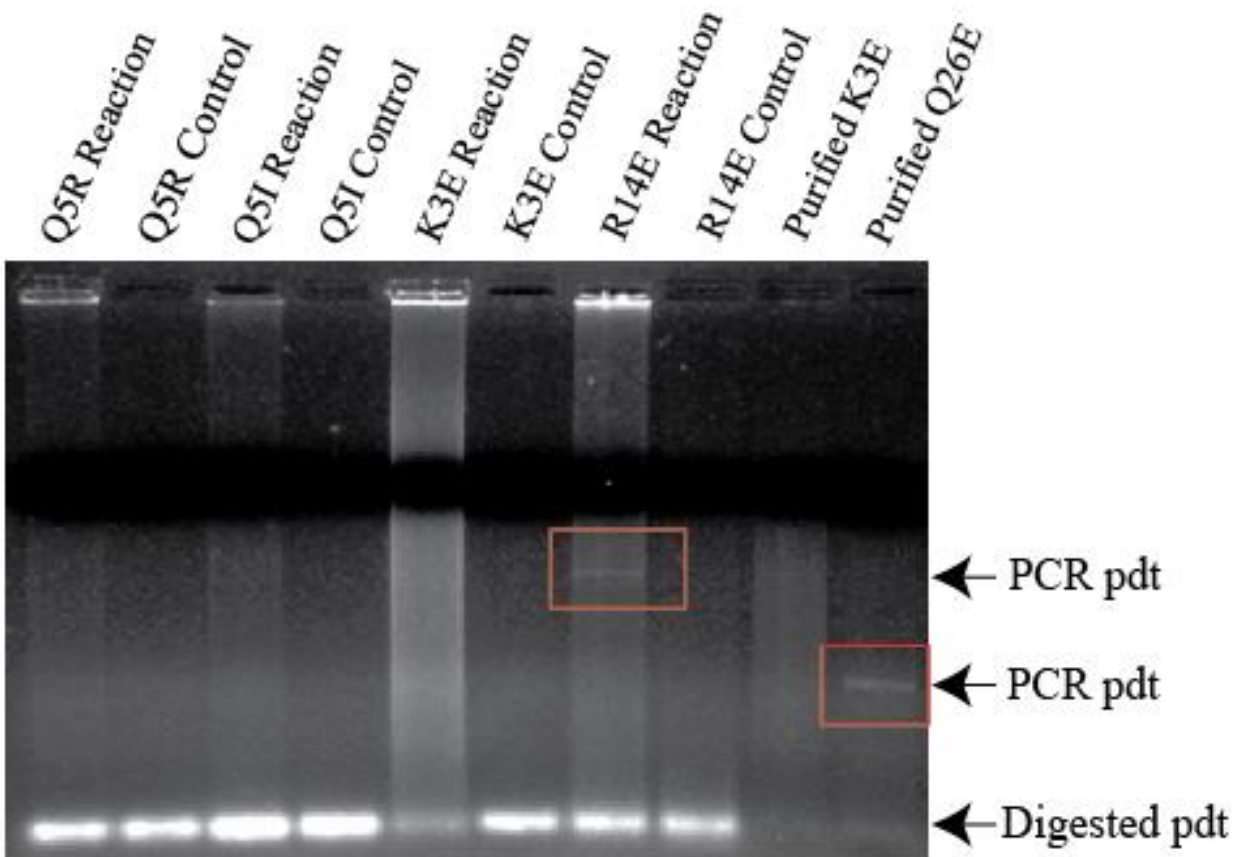

Figure 18: Gel image showing PCR product for R14E and Q26E

Successful Transformation of DH5-α E. coli with PCR Amplified DNA

For a successful transformation the expected result would be the growth of colonies on the agar plate. Figure 19 is an image of a successful transformation of mutant PLN Q26E into DH5-α E. *coli* as colonies grew. Mutant PLN R14E was also successfully transformed to DH5-α E. coli. However, K3E PLN was not successfully transformed. Given the success of mutant Q26E and R14E these two were focused on for the remainder of the laboratory study.
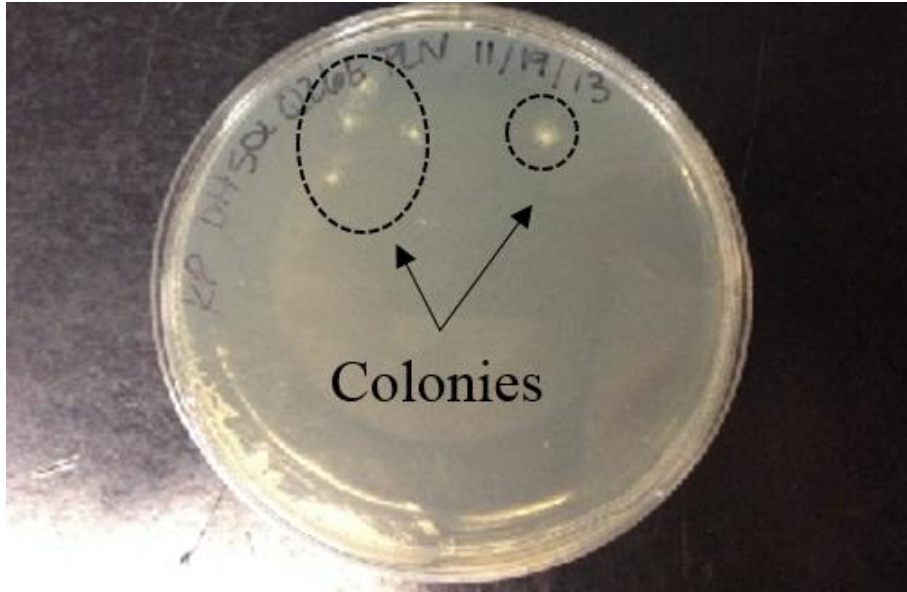
Figure 19: Colony growth of DH5-α E. coli containing Q26E PLN plasmid.

Quantification of Plasmid

Purified plasmids were quantified using UV-vis spectroscopy to measure absorbance at

260nm, and calculated the concentration using Beer's Law.

Mutant	Absorbance at 260nm	Concentration (ng/μL)
R14E	0.0662	36.41

Figure 20: R14E quantification data

Sequencing Data

The results of Sanger sequencing are below in figure 21, and the mutations are

highlighted in yellow.

Figure 21: Amino Acid Sequence for Transformed Samples

Each letter represents an amino acid. AFA-PLN was successfully cloned as the sequence matches that of wild-type PLN exactly, except where cysteine substitutions were expected. Both R14E and Q26E were compared for changes in the amino acid sequent to the AFA PLN sequence. Mutated R14E PLN was also successfully cloned as the sequence shows a substitution of glutamic acid at location 14 for arginine. Additionally, mutant Q26E PLN shows a substitution in the sequence of glutamic acid at position 26, and therefore was successfully cloned.

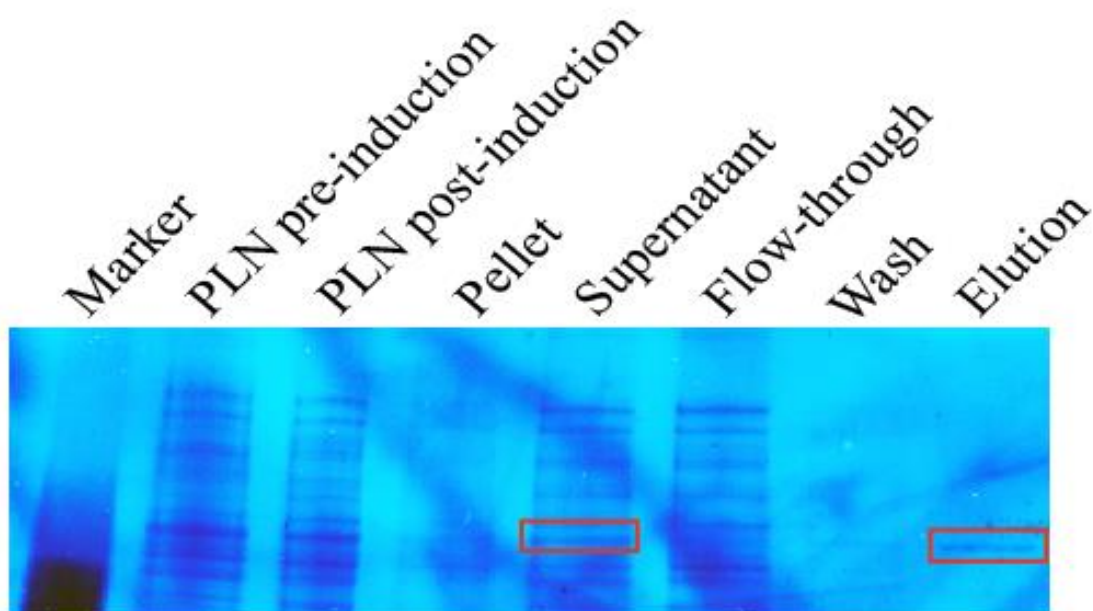***Purification by Affinity Column***

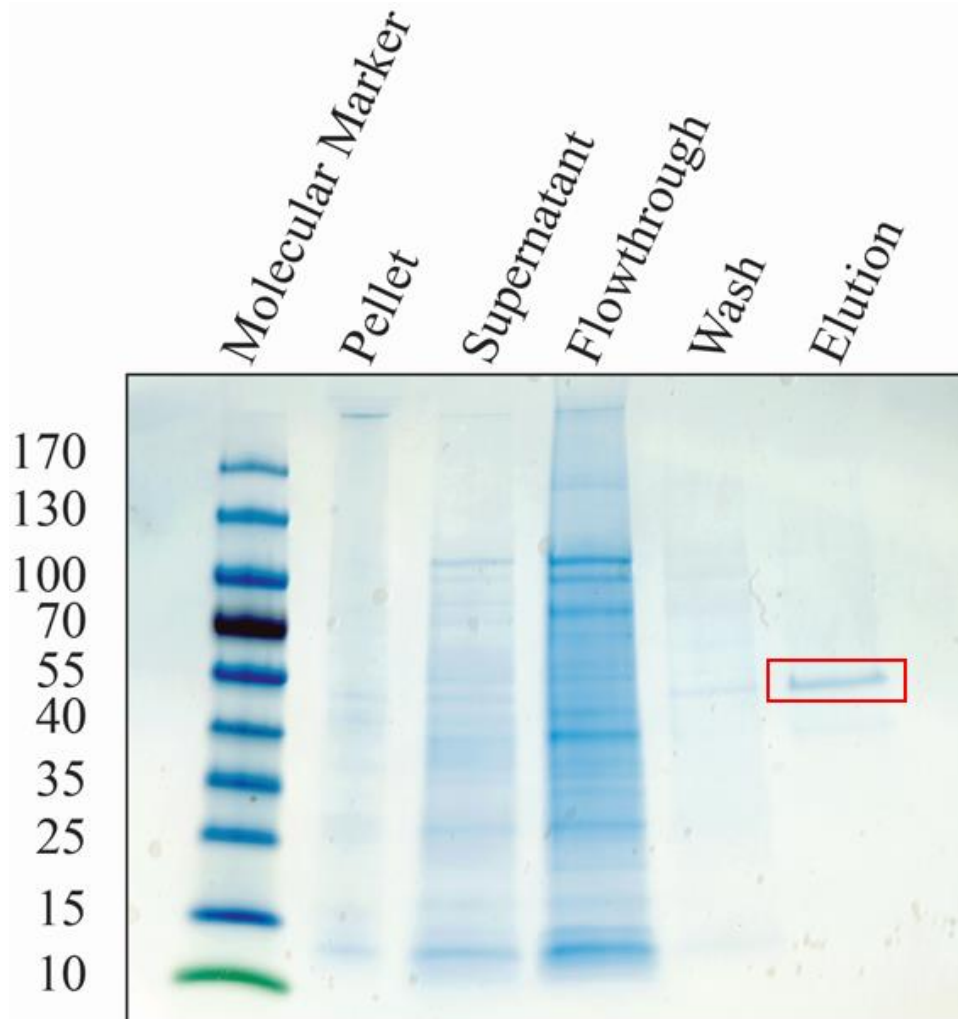*Figure 22: SDS-PAGE gel image for Q26E affinity chromatography*

Figure 23: SDS-PAGE gel image for R14E affinity chromatography

Figures 22 and 23 shows the results of the Q26E and R14E SDS-PAGE gels run after the respective affinity columns. In each gel there is a single band in the elution column, representing the desired mutant PLN protein fused to MBP. Figure 22 demonstrate the presence of the protein band in the elution, representing the PLN-MBP protein, in the supernatant, but not in the flow-though. There are corresponding bands the post-induction lane because the protein would begin to be expressed. There is also a band present in the pre-induction lane. Comparing the elution

band to the molecular marker in Figure 23 shows the eluted protein is around 50kDa, which is

the molecular weight of PLN-MBP.

DISCUSSION

Through this research, the predicted secondary structure, hydropathicity, and disorder of

each of rationally designed phospholamban mutants were analyzed. Additionally, two of these

mutants, Q26E and R14E, were successfully cloned and expressed. These mutants have been

purified with affinity chromatography and they are ready for final isolation, gel assays, and

further assessment. Originally, R14E was designed as part of a double mutant, K3E/R14E,

however, due to the timeline and interest in further processes beyond PCR, it was decided to

pursue study of the single R14E mutant.

The bioinformatics analysis provided helpful insight into potential properties of each of

the rationally designed mutants. Results of this analysis offered information to make a general

comparison to the five criteria for rationally designed therapeutic PLN mutants. Jpred3[37]

seemed to be an accurate bioinformatics tool as it showed two helices connected by a loop in WT

PLN, which is supported by literature. Secondary structure analysis by Jpred3[37] suggests that

each of these PLN mutants will retain their ability to bind SERCA, as minimal change to

secondary structure was observed. An ability to bind to SERCA is important for the mutant to

have an impact on SERCA affinity, or to potentially compete with wild-type PLN.

The Innovagen AB Hydropathicity[38] analysis was also an accurate model as it illustrates

the known amphipathic helix pattern and showed the correct local changes in charge due to

substitution. The amphipathic helix pattern can be seen by the hydropathicity switches between

hydrophobic and hydrophilic every three to four residues. The plot illustrates the localized

change based on each mutation, and the point amino acid substitution was represented in the

correct location in each diagram. Specifically, mutant K3E/R14E showed the largest deviation from WT PLN with a lower pKa value; therefore, the carboxylic acid in the R group would be deprotonated at biological pH. Prior to the mutation, the R group consists of a positive amino group at biological pH. Therefore, this change in charge from negative to positive likely will disrupt interactions and the helical pattern, leading to disorder in the structure. Increased disorder has the potential to mimic the phosphorylated state of PLN, which is the desired state as it relieves SERCA inhibition.

Disorder is important to assess in PLN mutants as it appears that the success of therapeutic PLN mutant S16E is largely in part to the increased structural dynamics exhibiting pseudo-phosphorylation, thus relieving SERCA inhibition.[21] Analysis by DisEMBLE[39] appears to be a valuable and accurate tool to predict disorder as the result showed an accurate disorder prediction for wild-type PLN as supported by literature. Increased structural dynamics are predicted in the known loop region, residues 10-20, for wild-type PLN.

As hypothesized, the double mutant, K3E/R14E is predicted to exhibit an increase in disorder (Figure 15). In fact, K3E/R14E is predicted to have the largest increase in disorder of the mutants here. PLN mutant Q26E however, showed similar disorder to WT PLN. Yet, in comparing the predicted mobility in the hot loops graph, PLN mutant Q26E showed an increase in structural dynamics in the loop region, as hypothesized. Since residue 26 is quite close to the hinge residue, number 21, it is likely that a change at position 26 will have an impact on the mobility due to proximity to residue 21. Additionally, Q26 is thought to swing away during phosphorylation; the substitution may result in an ability to swing more freely, potentially mimicking the phosphorylated state.[13] While further study was not pursued because of the lack of PCR success, Q5R is an interesting mutant for continued study as it is predicted to exhibit an

increase in mobility—which was hypothesized and predicted by DisEMBLE.[39] Mutant K3E/R14E is predicted to exhibit a slight decrease in mobility. With a change from positive to negative charge at two residues in domain 1a, the substituted residues likely may interact with amino acids which it previously repelled, potentially resulting in stiffness and a decrease in mobility. However, K3E/R14 still appears useful for further study because of the significant predicted increase in disorder. These findings are significant as increased disorder and increased mobility as predicted here is thought to mimic the phosphorylated state of PLN, which would relieve SERCA inhibition and is a desired criteria for therapeutic PLN mutant design.

Polymerase chain reaction can be a tricky procedure to have success with, even when being very careful and following the procedure accurately. This is likely why some, but not all, of the PCRs here worked. Also, PCR success attests to the quality of primer design.

As the PCR gels in figures 18 and 19 show, the bands were not always clear. For this reason, PCR purification was used before transformation—which seemed to improve the success of transformation. Like the PCR's, not all transformations were successful, so it was quite rewarding to transform two mutants.

While it was not expected to see a band for the elution protein in the pre-induction lane, there are two possible reasons accounting for this. The elution protein, PLN-MBP is 48kDa, which is near the average size for proteins, 50kDa. Therefore, it would not be unlikely that there is an endogenous protein of this molecular weight appearing in the pre-induction lane. Additionally, due to the consistency of the samples before put on the column, this particular gel is difficult to run, which could have affected the bands visible in the pre-induction lane. Overall, it does offer helpful and accurate information on the presence of the elution protein. Only one,

clear, band is visible in the elution column—supporting the expression and purification of the desired mutant protein.

The successful PCR and transformation of R14E and Q26E, as confirmed by sequencing data, is a promising result for further study of each of these mutants. It is possible to clone, transform, and express PLN mutants R14E and Q26E as confirmed by the affinity SDS PAGE gels (Figures 22 and 23). In fact, these mutants are the first successful mutants cloned and expressed in the last year in the biochemistry lab at St. Catherine University. Furthermore, these mutants possess properties predicted to fit three of the five criteria for PLN therapeutic mutant design as assessed thus far. Both PLN mutants demonstrated minimal change to the secondary structure, increase in disorder or mobility, and potential to be phosphorylated by PKA.

One of the goals in designing mutants for this project was to balance making enough change to affect the function of PLN, but not too much to inhibit interaction with SERCA or the main regulatory enzymes. Minimal change in the secondary structure is thought to be important for retaining the ability to interact with SERCA and the main regulatory enzymes of PLN, thus preserving some modulation of activity. On the other hand, increased disorder and mobility is thought to reduce or relieve PLN inhibition on SERCA. Both of the expressed mutants R14E and Q26E appear to achieve this balance as assessed thus far.

Mutant PLN Q26E preserves the availability of residue 16 to be phosphorylated, maintaining some biological control of the system. While it seems unlikely that mutant R14E may retain the ability to be phosphorylated by PKA because residue 14 is contained in the minimum recognition sequence, there is a possibility that it may. Preliminary studies suggest that R14Del does retained the ability to be phosphorylated at S16, however, very slowly.[41] Therefore, changing the residue at position 14 may still allow for phosphorylation by PKA at

S16. Additionally, these observations support that mutated peptide sequences of PLN as opposed to the whole protein also retain the ability to be phosphorylated slowly. The ability to be phosphorylated more slowly could be a desirable trait to still allow modulation of activity, but to still reduce the inhibition on SERCA.

CONCLUSION

Through this project, four PLN mutants were designed, and four questions were asked about these mutants—including effect on disorder and mobility; ability to be cloned, expressed, and purified; interaction with regulatory enzymes; and fit compared to the five criteria for PLN therapeutic mutant design. It was hypothesized that each mutant would retain a similar secondary structure, exhibit increased disorder or mobility, and that at least one mutant would be able to be cloned, expressed, and purified. Bioinformatics data analysis of secondary structure, hydropathicity, and disorder; PCR-site-directed mutagenesis; transformation of and expression with E. *coli* cells, were used to provide information and results for each question.

Bioinformatics analysis predicts each of the mutants will exhibit minimal to no change in secondary structure, as hypothesized, suggesting the ability to still interact with main regulatory enzymes and with SERCA. Mutants R14E and Q26E emerged as valuable not only because they are predicted by DisEMBLE[39] to exhibit increased disorder or mobility compared to WT PLN, but because they were each cloned, expressed, and purified. The other mutants, with the exception of Q5R, generally are predicted to possess similar or decreased disorder or mobility compared to WT PLN. In future related projects, these selected bioinformatics databases and properties for assessment could be useful to analyze a wide range of mutants in order to narrow down the options of potential mutants to pursue further study with in lab.

Through this project, rationally designed PLN mutants were assessed via bioinformatics and laboratory study. Three of the initial questions asked, number one, two, and four, were answered at least in part. Insight was provided to: 1) How might each of the rationally designed mutants affect the disorder and mobility of PLN? According to the bioinformatics results, the disorder or mobility of R14E and Q26E is predicted to increase. The following question was also answered: 2) Can the PLN mutants be effectively cloned, expressed, and purified? Both R14E and Q26E were effectively cloned, expressed, and purified. And last, predictions regarding the question four were assessed: 4) Do the PLN mutants meet the criteria for a PLN therapeutic mutant design? These two mutants, R14E and Q26E are predicted to meet three of the five criteria for PLN therapeutic mutant design.

As a result, these two mutants appear promising to pursue further research with. Both the R14E and Q26E mutants have been expressed by BL21 E. *coli* cells, purified with affinity chromatography, concentrated, and are ready for final isolation and further study. Additional analysis can seek to assess the interaction between each mutant and the main PLN regulatory enzymes. Assessment of the interaction and impact of these mutants on the affinity of SERCA for calcium ions is also an important area for future study. In addition, the mutant can further, and more closely, be compared against the therapeutic PLN mutant criteria. Further assessment of the impact and interaction of each of these two mutants with SERCA could offer insight into PLN and SERCA's role and relation to heart failure; as well as provide potential targets for gene therapy to treat heart failure.

REFERENCES

[1] Center for Disease Control and Prevention. (2013). *Heart Disease Fact Sheet*. Retrieved from
http://www.cdc.gov/dhdsp/data_statistics/fact_sheets/fs_heart_disease.htm

[2] American Heart Association. (2013). *Heart Failure*. Retrieved from
http://www.heart.org/HEARTORG/Conditions/HeartFailure/HeartFailure_UCM_00201
_SubHomePage.jsp

[3] Medeiros, A., Biagi, D.G., Sobreira, T.J.P., L. de Oliveira, P.S., Negrao, C.E., Mansur, A.J.,
Krieger, J.E., Brum, P.C., & Pereira, A.C. (2011). Mutations in the human
phospholamban gene in patients with heart failure. *American Heart Journal*, 162 (6),
1088-1095.

[4] Hall M.J., Levant S., & DeFrances C.J. (2012). Hospitalization for congestive heart failure:
United States, 2000–2010. National Center for Health Statistics, 108. Retrieved from
http://www.cdc.gov/nchs/data/databriefs/db108.htm#summary

[5] Iwanaga, Y., Hoshijima, M., Gu, Y., Iwatate, M., Dieterlie, T., Ikeda, Y., Date, M., Chrast, J.,
Matsuzaki, M., Peterson, K.L., Chien, K.R., Ross, J. (2004). Chronic phospholamban
inhibition prevents progressive cardiac dysfunction and pathological remodeling after
infarction in rats. *The Journal of Clinical Investigation*, 113, 727-736.

[6] National Institutes of Health U.S. National Library of Medicine. (2013). *Genetics Home
Research*. Retrieved from http://ghr.nlm.nih.gov/handbook/therapy/genetherapy

[7] Edes, I. & Kranias, E.G. (1989). Regulation of cardiac sarcoplasmic reticulum
function by phospholamban. *Membrane Biochemistry,* 7, 175-192.

[8] Khan Academy. (2013). *Heart muscle contraction.* Retrieved from
http://www.khanacademy.org/science/healthcare-and-medicine/heart-muscle-
contraction/v/calcium-puts-myosin-to-work

[9] Marks, A R. (2013). Calcium cycling proteins and heart failure: mechanisms and
therapeutics. *The Journal of Clinical Investigation*, 123, 46-52.

[10] Mattiazzi, A., & Kranias, E.G. (2011). CAMKII regulation of phospholamban
and SR Ca^{+2}lLoad. *Hearth Rhythm,* 8, 784-787.

[11] Lehman, W., Craig, R. & Vibert, P. (1994). Ca^{2+}-induced tropomyosin movement in
Limulus thin filaments revealed by three-dimensional reconstruction. *Nature,* 368 65-67.

[12] Schmitt, J.P., Kamisago, M., Asahi, M., Li, G.H., Ahmad, F.,Mende, U., Kranias, E.G.,
MacLennan, D.H., Seidman, J.G., Seidman, C.E. (2003). Dilated cardiomyopathy and
heart failure caused by mutation in phospholamban. *Science*, 299, 1410-1413.

[13] Ha, K.N., Traaseth, N.J., Verardi, R., Zamoon, J., Cembran, A., Karim, C.B., Thomas, D.D., & Veglia, G. (2007). Controlling the inhibition of the sarcoplasmic Ca^{2+}-ATPase by tuning phospholamban structural dynamics. *Journal of Biological Chemistry,* 282, 37205-37214.

[14] Hajjar, R.J., Monte, F.D., Matsui, T., & Rosenzweig, A. (2000). Prospects for gene therapy for heart failure. *Circulation Research*, 86, 616-621.

[15] Katz, A.M., Lorell, B.H. (2000). Regulation of cardiac contraction and relaxation. *Circulation,*102, IV-69-IV-74.

[16] Kranias, E.G. & Hajjar, R.J. (2012). Modulation of cardiac contractility by the phospholamban/SERCA2a regulatome. *Circulation Research*, 110, 1646-1660.

[17] Protein Data Bank. (2013). *PDB2KYV.* Retrieved from http://www.rcsb.org/pdb/explore.do?structureId=2KYV

[18] Bhupathy, P., Babu, G.J., & Periasmy, M. (2007). Sacrolipin and phospholamban as regulators of cardiac sarcoplasmic reticulum Ca^{+2} ATPase. *Journal of Molecular and Cellular Cardiology*, 42, 903-911.

[19] MacLennan, D.H., Kranias, E.G. (2003). Phospholamban: A Crucial regulator of cardiac contractility." *Molecular Cell Biology,* 4, 566-577.

[20] Lou, W., Grupp, I.L., Harrer, J., Ponniah, S., Grupp, G., Duffy, J.J., Doetschman, T., Kranias, E.G. (1994). Targeted ablation of the phospholamban gene is associated with markedly enhanced myocardial contractility and loss of beta-agonist stimulation. *Circulation Research,* 7, 401-409.

[21] Lockamy, E.L., Cornea, R.L., Karim, C.B., Thomas, D.D. (2011). Functional and physical competition between phospholamban and its mutants provides insight into the molecular mechanism of gene therapy for heart failure. *Biochemical and Biophysical Research Communication*, 408, 388-392.

[22] Kaye, D.M., Preovolos, A., Marshall, T., Byrne, M., Hoshijima, M., Hajjar, R., Mariani, J.A., Pepe, S., Chien, K.R., and Power, J.M. (2007). Percutaneous cardiac recirculation-mediated gene transfer of an inhibitory phospholamban peptide reverses advanced heart failure in large animals. *Journal of the American College of Cardiology,* 50, 253–260.

[23] Sarcoplasmic reticulum. (2013). In *Encycolpaedia Britannica Online.* Retrieved from http://www.britannica.com/EBchecked/topic/524096/sarcoplasmic-reticulum

[24] Smith, S.O., Kawakami, T., Liu, W., Zilox, M., & Aimoto, S. (2001). Helical structure of phospholamdan in membrane bilayers. *Journal of Molecular Biology*, 313, 1139-1148.

[25] Arkin, I.T., Adams, P.D., Brunger, A.T., Smith, S.O., & Engelman, D.M. (1997). Structural perspectives of phospholamban, a helical transmembrane pentamer. *Annual Review of Biophysics and Biomolecular Structure* 26, 157-179.

[26] Gustavasson, M., Traaseth, N.J., Karim, C.B., Lockamy, E.L.,Thomas, D.D., & Veglia, G. (2011). Lipid-Mediated folding/unfolding of phospholamban as a regulatory mechanism for the sarcoplasmic reticulum Ca^{2+} –ATPase. *Journal of Molecular Biology,* 408, 755-765.

[27] Sugita, Y., Miyashita, N., Yoda, T., Ikeguchi, M., Toyoshima, C. (2006). Structural changes in the cytoplasmic domain of phospholamban by phosphorylation at Ser16: A molecular dynamics study." *Biochemistry,* 45, 11752-11761.

[28] Ha, K.N., Gustavsson, M., Veglia, G. (2012). Tuning the structural coupling between the transmembrane and cytoplasmic domains of phospholamban to control sacrcoplasmic reticulum Ca(2+)-ATPase (SERCA) function. *Journal of Muscle Research and Cell Motility*, 33, 485-492.

[29] Ha, K.N. (2012). *Rational design of loss-of-function phospholamban mutants to tune SERCA function*. (Doctoral Dissertation). Available from University of Minnesota Dissertations. http://purl.umn.edu/126216

[30] Kimura Y., Asahi, M.. (1998). Sarcoplasmic reticulum Ca2+-ATPase isoform of cardiac influence functional interactions with the phospholamban domain Ib mutations. *Journal of Biological Chemistry,* 273, 14238-14241.

[31] Traaseth, N.J., Shi, L., Verardi, R., Mullen, D.G., Barany, G., Veglia, G. (2009). Structure and topology of monomeric phospholamban in lipid membranes determined by a hybrid solution and solid-state NMR approach. *Proceedings of the National Academy of Science,* 106 (25), 10165-10170.

[32] Toyoshima, C., Asahi, M., Sugita, Y., Khanna, R., Tsuda, T.,MacLennan, D.H. (2003). Modeling of the inhibitory interaction of phospholamban with the Ca^{2+} ATPase. *Proceedings of the National Academy of Science*, 100, 467-472.

[33] He, H., Meyer, M., Martin, J.L., McDonough, P.M., Ho, P., Lou, X., Lew, W.Y.W., Hilal Dandan, R., Dillmann, W.H.. (1999). Effects of mutant and antisense RNA of phospholamban on SR Ca+2-ATPase activity. *Circulation*, 100, 974-980.

[34] DeWitt, M.M., MacLeod, H.M., Soliven, B., McNally, E.M. (2006).Phospholamban R14 deletion results in late-onset, mild, hereditary, dilated cardiomyopathy. *Journal of the American College of Cardiology*, 48 (7), 1396-1398.

[35] Traaseth, N.J., Ha, K.N., Verardi, R., Shi, L., Buffy, J.J., Masterson, L.R., Veglia, G. (2008). Structural and dynamic basis of phospholamban and sarcolipin inhibition of Ca(+2)-ATPase. *Biochemistry*, 47, 3-13.

[36] Gustvasson, M., Verardi, R., Mullen, D.G., Mote, K.R., Traaseth, N.J., Gopinath, T., & Veglia, G. (2013). Allosteric regulation of SERCA by phosphorylation-mediated conformational shift of phospholamban. *Proceedings of the National Academy of Sciences and the United States of America*, Early Edition.

[37] Cole C, Barber JD & Barton GJ. (2008). Jpred 3: *Nucleic Acids Res.* The Barton Group, University of Dundee. Retrieved from http://www.compbio.dundee.ac.uk/www-jpred/

[38] Innovagen AB. (2012). http://www.innovagen.se/custom-peptidesynthesis/peptide-property calculator/peptide-property-calculator.asp

[39] Linding R., Jensen L.J., Diella F., Bork P., Gibson T. J. and R.B. Russell. (2003). Protein disorder prediction: implications for structural proteomics. *Structure,* 11. Retrieved from http://dis.embl.de/

[40] Veglia, G., Ha, K.N., Shi, L., Verardi, R., Traaseth, N.J. (2010). What can we learn from a small regulatory membrane protein? *Methods in Molecular Biology*, 654, 303-319.

[41] Kim, J., Veglia, G. (2014). Dynamics of R14E in study with protein kinase A. In preparation.